

See discussions, stats, and author profiles for this publication at:  
<https://www.researchgate.net/publication/5797908>

# ATP Synthesis by Decarboxylation Phosphorylation

**ARTICLE** *in* RESULTS AND PROBLEMS IN CELL DIFFERENTIATION ·  
FEBRUARY 2008

DOI: 10.1007/400\_2007\_045 · Source: PubMed

---

CITATIONS

14

---

READS

25

**2 AUTHORS**, INCLUDING:



**Christoph von Ballmoos**

Universität Bern

**38 PUBLICATIONS 1,103**

CITATIONS

SEE PROFILE

# ATP Synthesis by Decarboxylation Phosphorylation

Peter Dimroth (✉) · Christoph von Ballmoos

Institute of Microbiology, ETH Zürich,  
Wolfgang-Pauli-Strasse 10, 8093 Zürich, Switzerland  
[dimroth@micro.biol.ethz.ch](mailto:dimroth@micro.biol.ethz.ch)

**Abstract** Adenosine triphosphate (ATP) is used as a general energy source by all living cells. The free energy released by hydrolyzing its terminal phosphoric acid anhydride bond to yield ADP and phosphate is utilized to drive various energy-consuming reactions. The ubiquitous  $F_1F_0$  ATP synthase produces the majority of ATP by converting the energy stored in a transmembrane electrochemical gradient of  $H^+$  or  $Na^+$  into mechanical rotation. While the mechanism of ATP synthesis by the ATP synthase itself is universal, diverse biological reactions are used by different cells to energize the membrane. Oxidative phosphorylation in mitochondria or aerobic bacteria and photophosphorylation in plants are well-known processes. Less familiar are fermentation reactions performed by anaerobic bacteria, wherein the free energy of the decarboxylation of certain metabolites is converted into an electrochemical gradient of  $Na^+$  ions across the membrane (decarboxylation phosphorylation). This chapter will focus on the latter mechanism, presenting an updated survey on the  $Na^+$ -translocating decarboxylases from various organisms. In the second part, we provide a detailed description of the  $F_1F_0$  ATP synthases with special emphasis on the  $Na^+$ -translocating variant of these enzymes.

## 1

### Introduction

Adenosine triphosphate (ATP) is used as a general source of chemical energy by all living cells. The free energy released in hydrolyzing its terminal phosphoric anhydride bond to yield ADP and phosphate is utilized to drive various energy-consuming reactions, e.g., biosyntheses, membrane transport, regulatory networks, mechanical movements, nerve conduction, etc. Accordingly, the demand for ATP is impressive, amounting to a daily turnover of 50 kg in a human on average. In order to maintain a constant supply of ATP and to complete the cell energy cycle, its terminal phosphoric anhydride bond has to be continuously regenerated from ADP and phosphate. Individual cells may dispose of several distinct catabolic reaction sequences leading to ATP synthesis by substrate-level phosphorylation in the cytoplasmic compartment of the cell. The underlying mechanism involves storage of metabolic energy as an energy-rich phosphate bond and transfer of the phosphate moiety to ADP to yield ATP.

By far the greatest amount of ATP, however, is synthesized at the membrane by the ubiquitous  $F_1F_0$  ATP synthase. This multicomponent protein complex

is able to convert the free energy stored in an electrochemical gradient of protons or  $\text{Na}^+$  ions across the membrane into the high-energy phosphoric anhydride bond of ATP. While the mechanism of ATP synthesis by the ATP synthase itself is universal, distinct reactions are used by different cells or organelles to energize the membrane. In photosynthesis by plants, the thylakoid membrane of chloroplasts is energized by light to generate an electrochemical gradient of protons, and consequently ATP synthesis in these organelles is termed photophosphorylation. In mitochondria or aerobic bacteria, oxidation reactions drive proton flux through the respiratory chain complexes to charge the membrane, and ATP synthesis in these organelles or cells is therefore termed oxidative phosphorylation. Several anaerobic bacteria perform fermentation reactions, in which the free energy of the decarboxylation of a certain metabolite is converted into an electrochemical gradient of  $\text{Na}^+$  ions across the membrane. The thus stored energy is used to drive ATP synthesis in a process termed decarboxylation phosphorylation (for reviews see [Dimroth 1997, 2004](#); [Buckel 2001](#)). In this chapter we will focus on the latter mechanism. We will first give a state-of-the-art overview of the  $\text{Na}^+$ -translocating decarboxylases and succeed with a detailed description of the  $\text{F}_1\text{F}_0$  ATP synthases. Special emphasis will be given to  $\text{Na}^+$  translocation and torque generation by the  $\text{Na}^+$ -translocating variant of these enzymes.

## 2

## Fermentation Pathways with $\text{Na}^+$ -Transport Decarboxylases (NaT-DC)

### 2.1

#### Fermentation of Citrate

The fermentation of tri- or dicarboxylic acids by various bacteria includes a decarboxylation reaction which is coupled to  $\text{Na}^+$  translocation across the membrane (Dimroth 2004). This mode of energy conversion (Bush and Saier 2002) was first recognized for oxaloacetate decarboxylase of *Klebsiella pneumoniae* (Dimroth 1980, 1982a,b). The membrane-bound enzyme complex is induced during anaerobic growth on citrate, where it catalyzes a specific step of citrate metabolism. After uptake into the cell by the  $\text{Na}^+$ -dependent citrate carrier CitS (Pos and Dimroth 1996), citrate is cleaved by citrate lyase into acetate and oxaloacetate. The latter is subsequently converted to  $\text{CO}_2$  and pyruvate by the membrane-bound oxaloacetate decarboxylase sodium ion pump. Pyruvate is converted to acetyl-CoA and formate by pyruvate formate lyase, and part of the formate is cleaved to  $\text{CO}_2$  and  $\text{H}_2$  by formate hydrogen lyase. Acetyl-CoA is further metabolized to acetyl phosphate by phosphotransacetylase, and acetate kinase converts acetyl phosphate and ADP to acetate and ATP. A peculiarity of this pathway is the mode of synthesis of NAD(P)H for biosynthetic reactions. While most bacteria growing

fermentatively are faced with the problem of getting rid of reducing equivalents (mainly NADH) formed by the oxidation of the growth substrates, citrate fermentation by *K. pneumoniae* includes no oxidative steps and NADH is not generated. However, as the mean oxidation status of citrate is above average for cellular components, the cells require reducing equivalents for citrate assimilation. It has been shown that hydrogen generated in the formate hydrogen lyase reaction provides the reducing equivalents for NAD(P)H formation from NAD(P)<sup>+</sup> by a soluble or a membrane-bound hydrogenase (Steuber et al. 1999).

Overall, the citrate fermentation pathway produces 1 mol ATP per mol citrate by substrate-level phosphorylation in the acetate kinase reaction, and in addition, an electrochemical gradient of Na<sup>+</sup> ions is generated by the oxaloacetate decarboxylase. The chemical concentration gradient of Na<sup>+</sup> is used to drive citrate uptake by the electroneutral Hcitrate<sup>2-</sup>/Na<sup>+</sup>/H<sup>+</sup> symporter (CitS) (Pos and Dimroth 1996), and the electrical component of the  $\Delta\mu\text{Na}^+$  is assumed to contribute driving force for ATP synthesis by the H<sup>+</sup>-translocating F<sub>1</sub>F<sub>0</sub> ATP synthase, which is constitutively expressed in this organism.

In *K. pneumoniae*, the structural genes for oxaloacetate decarboxylase are part of the gene cluster for citrate fermentation, which comprises two operons (*citS* and *citC* operons) with divergent orientation (Bott and Dimroth 1994; Bott et al. 1995; Bott 1997). The *citS* operon includes the genes for the citrate carrier (*citS*), the three structural genes for oxaloacetate decarboxylase (*oadGAB*), and a two-component regulatory system (*citAB*). The genes of the *citC* operon encode citrate lyase ligase (*citC*), the three subunits of citrate lyase (*citDEF*), and an enzyme involved in the biosynthesis of its 2'-(5''-phosphoribosyl)-3'-dephospho-CoA prosthetic group (*citG*) (Schneider et al. 2000a,b). An additional gene required for the prosthetic group biosynthesis (*citX*) has been found at a distant location, clustered with the two-component regulatory system (*citYZ*) and another citrate carrier (*citW*) (Schneider et al. 2002).

Data bank searches revealed genes for oxaloacetate decarboxylase in numerous anaerobic bacteria and in some archaea. Some of these organisms even possess several oxaloacetate decarboxylase genes. In *Salmonella typhimurium*, two copies of the *oad* genes have been identified, one being inserted into the citrate fermentation operon and expressed during anaerobic growth on citrate, and the other being associated with genes required for tartrate fermentation and expressed under anaerobic growth on tartrate (Wifling and Dimroth 1989; Woehlke et al. 1992; Woehlke and Dimroth 1994). *Vibrio cholerae* also has two copies of the *oad* genes; the *oad-2* genes are part of the citrate fermentation operon and are expressed during anaerobic growth on citrate (Dahinden et al. 2005a). The *oad-1* genes are not associated with genes for a specific fermentation pathway and conditions for their expression are unknown. The archaeon *Archaeoglobus fulgidus* contains a cluster of three *oad* genes. The gene for the oxaloacetate specific carboxyltransferase sub-

unit is not part of this cluster but found at a separate location of the genome (Dahinden and Dimroth 2004). Furthermore, the genome contains a gene for a methylmalonyl-CoA specific carboxyltransferase. It is conceivable that these different carboxyltransferases form sodium ion translocating decarboxylase complexes with different substrate specificity, and share the three proteins that are encoded by the *oad* gene cluster.

## 2.2

### Fermentation of Succinate or Lactate

Methylmalonyl-CoA decarboxylase is another member of the NaT-DC enzyme family. It has been characterized in lactate fermenting *Veillonella parvula* (Hilpert and Dimroth 1982, 1983; Huder and Dimroth 1993) and in succinate fermenting *Propionigenium modestum* (Bott et al. 1997). The decarboxylase converts (S)-methylmalonyl-CoA to propionyl-CoA and CO<sub>2</sub> and conserves energy by coupling the exergonic decarboxylation reaction to the transport of Na<sup>+</sup> ions across the membrane. In both bacteria, methylmalonyl-CoA decarboxylation is an essential step in the metabolism of succinate to propionate and CO<sub>2</sub> (Dimroth and Schink 1998; Schink and Pfennig 1982). In spite of these similarities, only *P. modestum* but not *V. parvula* is able to grow from the conversion of succinate to propionate and CO<sub>2</sub>. In *V. parvula*, the conversion of succinate to propionate is part of the lactate fermentation pathway, which produces sufficient ATP for growth by substrate-level phosphorylation. ATP production by decarboxylation phosphorylation is therefore not mandatory in this organism, and its inability to grow on succinate may in fact be due to the lack of a suitable F<sub>1</sub>F<sub>0</sub> ATP synthase (Denger and Schink 1982).

*Propionigenium modestum* was the first bacterium shown to gain energy for growth exclusively from a decarboxylation reaction and is thus the paradigm for the mechanism of decarboxylation phosphorylation (Fig. 1) (Hilpert and Dimroth 1982; Hilpert et al. 1984). Succinate metabolism starts with the transfer of the CoA moiety from propionyl-CoA to succinate to yield succinyl-CoA and propionate. Rearrangement of the carbon skeleton of succinyl-CoA with a B12-dependent enzyme leads to (R)-methylmalonyl-CoA, which is subsequently converted to (S)-methylmalonyl-CoA. The membrane-bound (S)-methylmalonyl-CoA decarboxylase conserves energy by coupling the decarboxylation reaction to the transport of Na<sup>+</sup> ions across the membrane. The product propionyl-CoA is used to activate a new succinate molecule to succinyl-CoA. The energy stored in the electrochemical gradient of Na<sup>+</sup> ions is subsequently used to drive ATP synthesis by a Na<sup>+</sup>-translocating F<sub>1</sub>F<sub>0</sub> ATP synthase. Given the bioenergetic demands for ATP synthesis in growing bacteria (~60 kJ/mol) (Thauer et al. 1977) and the free energy of the decarboxylation reaction (~ - 20 kJ/mol) (Schink and Pfennig 1982), it is clear that approximately three rounds of succinate degradation are required to support the synthesis of one molecule of ATP. The bioener-

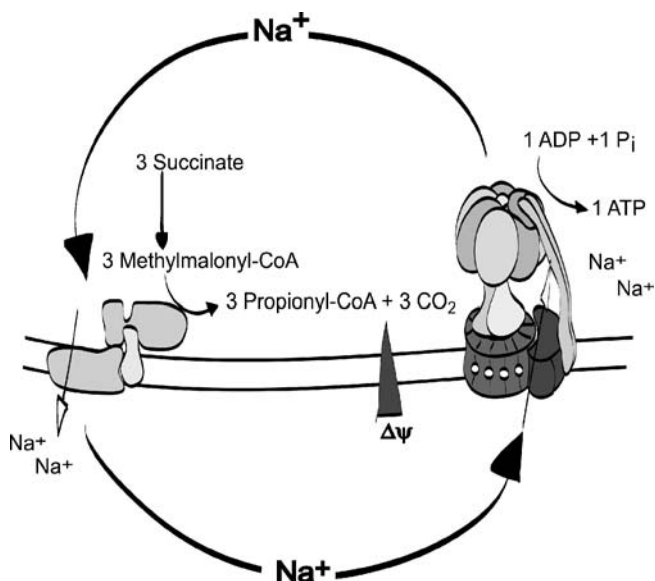


**Fig. 1** ATP synthesis by decarboxylation phosphorylation in *P. modestum*

getic relationships require a proper adjustment of the ratios between chemical reaction and Na<sup>+</sup> translocation of the two membrane-bound complexes operating in tandem. Methylmalonyl-CoA decarboxylase has been shown to translocate one Na<sup>+</sup> ion electrogenically and one Na<sup>+</sup> ion electroneutrally (in exchange for H<sup>+</sup>) across the membrane per decarboxylation event (Hilpert and Dimroth 1991; DiBerardino and Dimroth 1996). For the synthesis of one molecule of ATP, 3.3 Na<sup>+</sup> ions need to traverse the ATP synthase electrogenically (Stahlberg et al. 2001; Dimroth and Cook 2004). These ratios thus perfectly match the requirements for ATP synthesis by decarboxylation phosphorylation in *P. modestum*.

## 2.3

### Fermentation of Malonate

Anaerobic malonate degrading bacteria are yet another example for the in vivo ATP synthesis by decarboxylation phosphorylation. A representative of this class of organisms is *Malonomonas rubra* which grows fermentatively on malonate by converting it to acetate and CO<sub>2</sub> (Dehning and Schink 1989). Malonate uptake into the cell has been shown to be catalyzed by a transporter consisting of two different subunits (MadL and MadM). The transported species is Hmalonate<sup>-</sup> and this is taken up in an electroneutral symport with one Na<sup>+</sup> ion into the cell (Schaffitzel et al. 1998). Free malonate is chemically inert, and therefore the malonate degrading enzyme machinery (Hilbi et al.

1992; Dimroth and Hilbi 1997) harbors an activation module with a built-in acetyl thioester residue on a 2'-(5''-phosphoribosyl)-3'-dephospho-CoA prosthetic group on an acyl carrier protein (acetyl-ACP) (Berg et al. 1996, 1997). This device serves to transfer the ACP moiety from acetate to malonate in the first partial reaction, thus generating the activated malonyl-ACP species and acetate. The degradation continues with the transfer of the free carboxyl group of malonate to the prosthetic biotin group of a small biotin carrier protein (Berg and Dimroth 1998). The protein with the carboxybiotin residue diffuses to a membrane-bound decarboxylase, where the carboxybiotin is decarboxylated. This reaction is coupled to the transport of two  $\text{Na}^+$  ions out of the cell and a simultaneous uptake of one proton into the cell. As a result, one  $\text{Na}^+$  ion is exported from the cell electrogenically (together with a positive charge), but the other is exported electroneutrally (in exchange for  $\text{H}^+$ ). It can be envisaged that the latter recycles into the cell during malonate uptake by the electroneutral  $\text{Hmalonate}^-/\text{Na}^+$  symporter (Schaffitzel et al. 1998). The electrogenically exported  $\text{Na}^+$  ions are thought to energize ATP synthesis. Details of the ATP synthesizing enzyme of this bacterium have not yet been elucidated. The bioenergetic premises of ATP synthesis in *M. rubra*, however, are similar to those in *P. modestum*, requiring about three decarboxylation events to synthesize one molecule of ATP. *M. rubra* and *P. modestum* are two examples where ATP is exclusively synthesized by decarboxylation phosphorylation. These organisms are distinct with respect to the dicarboxylic acid degraded and the appropriate enzyme equipment needed to decarboxylate its specific substrate, but share the conservation of chemical energy as an electrochemical  $\text{Na}^+$  ion gradient.

## 2.4

### Fermentation of Glutarate

Decarboxylation phosphorylation is also the ATP-generating mechanism in *Pelospora glutarica*, a strictly anaerobic bacterium growing on glutarate as sole carbon and energy source (Matthies and Schink 1992a; Matthies et al. 2000). The metabolism of glutarate starts with its activation to glutaryl-CoA by CoA transfer from acetyl-CoA. Subsequently, the glutaryl-CoA is oxidized by a  $\text{NAD}^+$ -dependent dehydrogenase to glutaconyl-CoA. The key energy conserving reaction is the decarboxylation of glutaconyl-CoA to crotonyl-CoA by a membrane-bound biotin-containing  $\text{Na}^+$  pump that shares many properties with other members of the NaT-DC enzyme family. Reduction of crotonyl-CoA to butyryl-CoA with NADH regenerates the  $\text{NAD}^+$  consumed in the glutaryl-CoA dehydrogenase reaction, and CoA transfer to acetate produces butyrate and generates the acetyl-CoA consumed in the activation of glutarate. Part of the butyryl-CoA isomerizes to isobutyryl-CoA, before the CoA moiety is transferred to acetate, yielding acetyl-CoA and isobutyrate (Matthies and Schink 1992b). Glutaconyl-CoA decarboxylase is also a key en-

ergy converting reaction in the fermentation of glutamate by *Acidaminococcus fermentans*, and the enzyme from this source has been well characterized biochemically (Buckel and Semmler 1983; Buckel 2001).

### 3

#### Structure and Mechanism of the NaT-DC Enzymes

The NaT-DC enzyme family includes oxaloacetate decarboxylase, methylmalonyl-CoA decarboxylase, glutaconyl-CoA decarboxylase, and malonate decarboxylase. These are multisubunit protein complexes, composed of water-soluble and membrane-intrinsic components. The biotin prosthetic group of these enzymes accepts the CO<sub>2</sub> moiety from the substrate at the water-exposed carboxyltransferase site and delivers it to the membrane-bound decarboxylase site, where the decarboxylation is coupled to Na<sup>+</sup> ion transport across the membrane. Many fundamental investigations have been performed with the oxaloacetate decarboxylase, and we shall give a detailed account of this enzyme below.

#### 3.1

##### Oxaloacetate Decarboxylase Na<sup>+</sup> Pump

As described above, oxaloacetate decarboxylase of *K. pneumoniae*, *S. typhimurium*, or *V. cholerae* is encoded by the three structural genes *oadG*, *oadA*, and *oadB*, which are part of the *citS* operon within the citrate fermentation gene cluster (Woehlke et al. 1992). *oadG* codes for the  $\gamma$  subunit (8.9 kDa) which consists of an N-terminal hydrophobic  $\alpha$  helix serving as a membrane anchor and a water-soluble C-terminal domain, which is linked to the membrane domain by a flexible linker peptide consisting mainly of proline and alanine residues. The  $\gamma$  subunit plays an essential role in the complex formation of the decarboxylase, but appears to have no catalytic function by itself (Schmid et al. 2002a). Near the C terminus, the  $\gamma$  subunit contains a Zn<sup>2+</sup> metal ion (Dimroth and Thomer 1983; DiBerardino and Dimroth 1995). *oadA* codes for the water-soluble  $\alpha$  subunit (63.5 kDa) which has a three domain structure. The N-terminal domain, which harbors the carboxyltransferase catalytic site, is bound via a flexible proline/alanine-rich linker peptide to the association domain, which promotes complex formation with the  $\gamma$  subunit (Dahinden et al. 2005b). At its C terminus, another proline/alanine linker connects the association domain to the biotin domain with the prosthetic group bound to a lysine residue, 35 amino acid residues before the C terminus. The crystal structure of the carboxyltransferase shows a dimer of  $\alpha_8\beta_8$  barrels with an active site Zn<sup>2+</sup> ion at the bottom of a deep cleft that is liganded by an aspartate and two histidine residues (Studer et al. 2007). *oadB* codes for the  $\beta$  subunit (44.9 kDa), a very hydrophobic integral membrane protein that folds into a block of three



N-terminal membrane-spanning  $\alpha$  helices, a hydrophobic linker peptide, inserting into the membrane but not traversing it, and a block of six C-terminal membrane-spanning  $\alpha$  helices (Jockel et al. 1999).

A model of structure and function of the oxaloacetate decarboxylase  $\text{Na}^+$  pump is depicted in Fig. 2. The catalytic cycle starts with the transfer of the carboxylic group from oxaloacetate to the biotin prosthetic group on the enzyme. The carboxyl transfer reaction is proposed to follow a two-step sequence. First, the  $\text{Zn}^{2+}$  ion is thought to coordinate the carboxylate in position 4 of oxaloacetate to facilitate its transfer to the  $\epsilon$ -amino group of a conserved, essential, active site lysine residue. The biotin subsequently accepts the carboxyl group from the carbamoyl-lysine intermediate (Studer et al. 2007). Evidence for a carbamoyl-lysine was found in the crystal structure of the 5 S subunit of transcarboxylase which catalyzes exactly the same reaction as OadA (Hall et al. 2004). The carboxybiotin thus formed switches from the carboxyltransferase catalytic site to the decarboxylase site on OadB (Dimroth and Thomer 1983, 1993). It has been proposed that the  $\text{Zn}^{2+}$  on the C-terminal tail of the  $\gamma$  subunit coordinates the carboxyl group of carboxybiotin during the transfer to protect the chemically labile compound from spontaneous decarboxylation (Studer et al. 2007). At OadB the decarboxylation takes place, and the free biotin group is regenerated. During this  $\text{Na}^+$ -dependent reaction, a periplasmically derived proton is consumed and two sodium ions are translocated from the cytoplasm into the periplasm (DiBerardino and Dimroth 1996). Essential residues for this reaction have been identified by site-specific mutagenesis of OadB (Jockel et al. 2000a,b; Schmid et al. 2002b). Based on these studies and other biochemical investigations, a model for the reaction mechanism was proposed which is shown

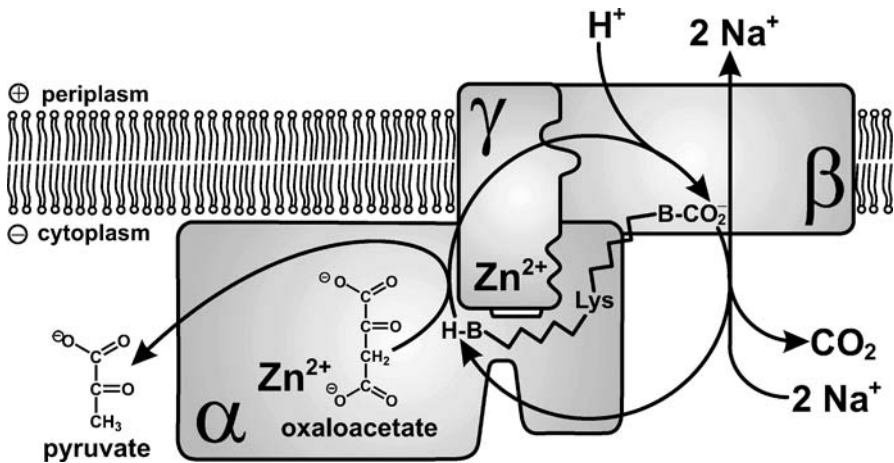


**Fig. 2** Model of structure and function of the oxaloacetate decarboxylase  $\text{Na}^+$  pump. (B-H, biotin;  $\text{B-CO}_2^-$ , carboxybiotin; Lys, biotin-binding lysine residue)

in Fig. 3. The model predicts that a number of highly conserved and functionally indispensable residues on helices IV and VIII and on region IIIa of OadB are involved in the ion translocation mechanism. At the decarboxylase site on OadB, the carboxybiotin is thought to form a stable complex, possibly with the side chain of R389 at the cytoplasmic surface of helix VIII. Site-

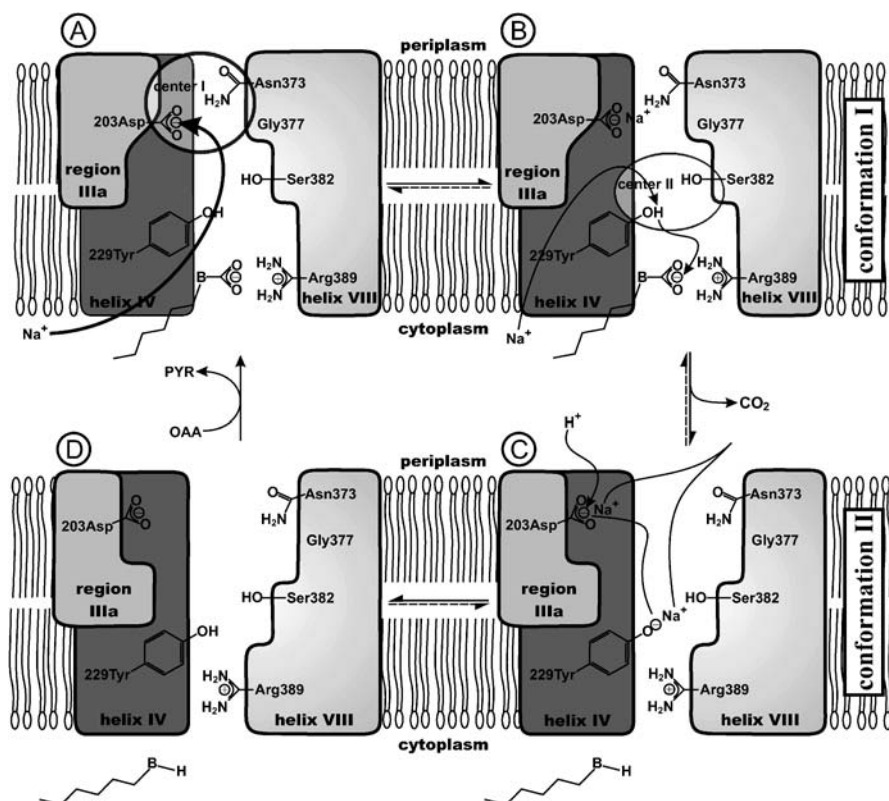


**Fig. 3** Model for decarboxylation of carboxybiotin and vectorial  $\text{Na}^+$  transport. The appropriate locations of important residues in helix IV, VIII, and in region IIIa of the  $\beta$  subunit and their participation in the  $\text{Na}^+$  transport mechanism are depicted. *Panel A* shows the empty binding site region with enzyme-bound carboxybiotin ( $\text{B-CO}_2^-$ ), exposing the  $\text{Na}^+$  binding sites toward the cytoplasm. In *panel B*, the first  $\text{Na}^+$  binding site at the D203-N373 pair has been occupied and the second  $\text{Na}^+$  enters the Y229-S382 site, displacing the phenolic proton from Y229 with a rearrangement of the hydrogen-bonding network. The proton delivered to the carboxybiotin causes the immediate decarboxylation of this acid labile compound. This elicits the conformational change ( $\text{B} \rightarrow \text{C}$ ) exposing the  $\text{Na}^+$  binding sites toward the periplasm. The ions are released into this reservoir and a proton enters the periplasmic channel and restores the hydroxyl group of Y229. In *panel D*, the  $\text{Na}^+$  binding sites are empty and exposed toward the periplasm and the biotin is not modified ( $\text{B} \rightarrow \text{H}$ ). Upon carboxylation of the biotin, the protein switches back into the conformation where the  $\text{Na}^+$  binding sites are exposed toward the cytoplasm ( $\text{D} \rightarrow \text{A}$ )

directed sulfhydryl labeling with methanethiosulfonate reagents has identified helix VIII to align the channel for  $\text{Na}^+$  and  $\text{H}^+$  conductance across the membrane (Wild et al. 2003). Evidently, the proton which moves from the periplasmic reservoir through this channel must reach the carboxybiotin near the cytoplasmic surface to account for the consumption of a proton in the decarboxylation reaction. According to the model (Schmid et al. 2002b), the  $\text{Na}^+$  channel is initially open to the cytoplasm. In this conformation, the two different  $\text{Na}^+$  binding sites are of high affinity ( $K_s \sim 1 \text{ mM}$ ). The first  $\text{Na}^+$  is thought to bind at a site near the periplasmic surface (center I), which includes the side chains of D203 and probably also of N373. Subsequently, the second  $\text{Na}^+$  binds to the Y229 and S382 including site (center II). At this integral membrane location (center II) the  $\text{Na}^+$  ion will only be tolerated after charge balancing, i.e., after dissociation and removal of a proton from the site. The proton from the phenolic hydroxyl group of Y229 is therefore assumed to dissociate as the  $\text{Na}^+$  ion is approaching and to move to the carboxybiotin, where it is consumed during decarboxylation of this acid-labile compound. Concomitantly, the biotin prosthetic group leaves the site and OadB changes its conformation. This exposes the  $\text{Na}^+$  binding sites toward the periplasm and simultaneously decreases their  $\text{Na}^+$  binding affinities. The  $\text{Na}^+$  ions dissociate into the periplasmic reservoir, while a proton enters the periplasmic channel and restores the hydroxyl group of Y229. Hence, each decarboxylation event is coupled to the transport of two  $\text{Na}^+$  ions from the cytoplasm to the periplasm and the consumption of a periplasmically derived proton.

The amino acid sequences of the membrane-embedded  $\beta$  subunits of the NaT-DC family are very similar, and therefore these partial enzymes are thought to act by a common reaction mechanism. Distinct primary structures are found, however, for the carboxyltransferase subunits/domains, suggesting that these partial enzymes operate by different mechanisms. The crystal structures of the carboxyltransferase of glutaconyl-CoA decarboxylase (Wendt et al. 2003) and oxaloacetate decarboxylase (Studer et al. 2007) are indeed not related to each other and indicate a different reaction mechanism for each of them.

## 4

### ATP Synthesis Energized by an Electrochemical $\text{Na}^+$ Ion Gradient

#### 4.1

#### $\text{H}^+$ - and $\text{Na}^+$ -Translocating ATP Synthases

The mechanism of decarboxylation phosphorylation is completed by the synthesis of ATP, utilizing the electrochemical gradient of  $\text{Na}^+$  ions as energy source. The enzyme responsible for ATP synthesis is a  $\text{Na}^+$ -translocating  $\text{F}_1\text{F}_0$  ATP synthase.  $\text{F}_1\text{F}_0$  ATP synthases are ubiquitous from bacteria to plants and

animals, but usually use  $H^+$  rather than  $Na^+$  as the coupling ion (Boyer 1993; Capaldi and Aggeler 2002; Dimroth et al. 2006). This is reasonable, since the oxidation of nutrients in animals or bacteria or photosynthesis in plants leads to the formation of an electrochemical proton gradient across the membrane. Some bacteria with a fermentative metabolism, e.g., *P. modestum*, *M. rubra*, or *P. glutarica*, synthesize ATP exclusively by decarboxylation phosphorylation, while others can synthesize ATP also by substrate-level phosphorylation. Detailed studies have been performed with the closely related ATP synthases from *P. modestum* and *Ilyobacter tartaricus*. The *P. modestum* enzyme was the first  $F_1F_0$  ATP synthase found to act with  $Na^+$  and not with  $H^+$  as the physiological coupling ion (Laubinger and Dimroth 1987, 1988, 1989). The advantage of this coupling ion specificity is to provide a direct link to the  $Na^+$ -translocating decarboxylase, completing the  $Na^+$  cycle without an intermediate interconversion of a  $Na^+$  into a  $H^+$  gradient with a  $Na^+/H^+$  antiporter. The ATP synthases of *P. modestum*, *I. tartaricus*, or *Escherichia coli* are encoded by eight structural genes that are organized in an operon (Krumholz et al. 1992; Kaim et al. 1992). The first gene of the operon, which is termed *i* gene, encodes an integral membrane protein that is not part of the ATP synthase complex. In an *i* gene deletion clone of *E. coli*, the cells were still able to synthesize ATP by the  $F_1F_0$  ATP synthase, albeit at a reduced level (Gay 1984). This suggests that the *i* gene product is not essential for the production of a functional ATP synthase complex, but that it might help to make the assembly more efficient. Downstream of the *i* gene are the structural genes for the ATP synthase, starting with the gene for subunit *a*. This is followed by the genes for the other membrane-bound subunits *c* and *b* and by the genes for the water-soluble subunits  $\delta$ ,  $\alpha$ ,  $\gamma$ ,  $\beta$ , and  $\epsilon$ . The similarity between the *atp* operons from *P. modestum* and *E. coli* allowed the construction of hybrid ATP synthases harboring parts from either bacterium (Kaim and Dimroth 1993, 1994). The hybrids were constructed in the *E. coli* strain CM1470 that carries a deletion in the genes for the ATP synthase subunits *a*, *c*, *b*,  $\delta$ , and part of  $\alpha$ . As this strain does not form a functional ATP synthase, it is unable to grow by oxidative phosphorylation with succinate as carbon source. This defect could be complemented by transformation with plasmid pAP42 which harbors those ATP synthase genes from *P. modestum* that were lacking on the chromosome of *E. coli* CM1470. As a result of homologous recombination, the *P. modestum* genes were integrated into the chromosome of *E. coli* CM1470, yielding the new strain *E. coli* PEF42, which synthesizes a functional ATP synthase hybrid and is thus able to grow on succinate minimal medium. These results impressively buttress the common origin of  $H^+$ - and  $Na^+$ -translocating  $F_1F_0$  ATP synthases. The  $Na^+$ -translocating ATP synthases occur exclusively in anaerobic bacteria. Other representatives of this class were found in *Acetobacterium woodii* (Müller et al. 2001) and in *Clostridium paradoxum* (Ferguson et al. 2006).

The  $F_1F_0$  ATP synthases are nanosize rotary engines, organized as an assembly of two entities,  $F_1$  and  $F_0$ , which are connected by a central and a peripheral

stalk (Fig. 4). Each of these protein complexes functions as a reversible rotary motor and exchanges energy with the opposite motor through mechanical rotation of the central stalk. During ATP synthesis, the electrochemical ion gradient fuels the membrane-embedded  $F_0$  motor to rotate the central stalk in its intrinsic direction. Conversely, ATP hydrolysis by the  $F_1$  motor causes reverse rotation of the shaft, which converts the  $F_0$  motor into an ion pump. Under normal circumstances, the  $F_0$  motor generates the larger torque and drives the  $F_1$  motor in the ATP synthesis direction. However, in fermenting bacteria, when the respiratory enzymes are not active, the  $F_1$  motor hydrolyzes ATP to use the  $F_0$  motor as the generator of the indispensable membrane potential. An interesting example is the anaerobic thermoalkaliphilic bacterium *C. paradoxum*

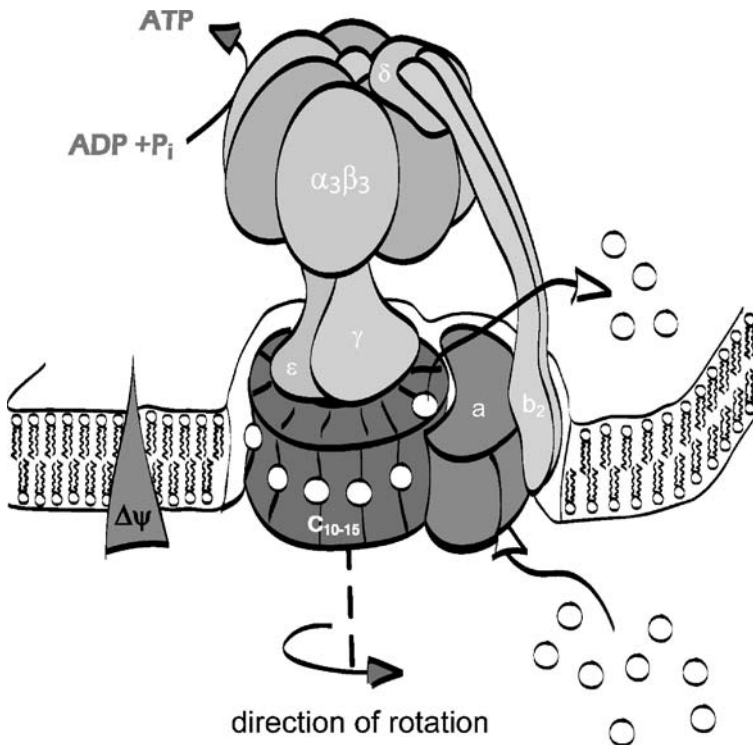


**Fig. 4** Cartoon of structure and function of a bacterial ATP synthase.  $F_1$  (subunits  $\alpha_3\beta_3\gamma\delta\epsilon$ ) and  $F_0$  (subunits  $a b_2 c_{10-15}$ ) are two motors that exchange energy by rotational coupling. The rotary subunits are  $\gamma\epsilon c_{10-15}$  and the membrane anchored and cytoplasmic stator subunits are  $a b_2 \alpha_3 \beta_3 \delta$ . During ATP synthesis, coupling ions (shown as white circles) pass through the  $F_0$  motor from the periplasm to the cytoplasm, inducing rotation and enabling the  $F_1$  motor to synthesize ATP

(Ferguson et al. 2006), which generates ATP in the fermentation of glucose to acetate and CO<sub>2</sub>, and uses these acids to keep the cytoplasmic pH near neutral in spite of the alkaline environment. The physiological function of the F<sub>1</sub>F<sub>0</sub> ATPase of this organism is to generate a membrane potential by hydrolyzing some of the ATP and in order to not compromise pH homeostasis, the ATPase uses Na<sup>+</sup> and not H<sup>+</sup> as the coupling ion.

## 4.2

### The F<sub>1</sub> Motor

For the F<sub>1</sub> motor, no differences between H<sup>+</sup>- and Na<sup>+</sup>-translocating ATP synthases have been reported so far. The motor consists of a hexameric assembly of alternating  $\alpha$  and  $\beta$  subunits around a central coiled-coil  $\gamma$  subunit. The F<sub>1</sub> complex is intrinsically asymmetric, owing to different interactions of the central  $\gamma$  subunit with each of the catalytic  $\beta$  subunits, and provides them with different conformations and nucleotide affinities at their catalytic sites. On rotation of the  $\gamma$  subunit, the conformations of the  $\beta$  subunits change sequentially such that each  $\beta$  subunit adopts the same conformations of varying affinity during one rotational cycle. As a result, three molecules of ATP are synthesized. This model, known as the binding change mechanism (Boyer 1993), explains a wealth of biochemical and kinetic data. Important details of this mechanism, however, are still under active investigation. The rotational model is consistent with the crystal structure of F<sub>1</sub>, which shows a marked asymmetry in the conformations and nucleotide occupancy of the catalytic  $\beta$  subunits (Abrahams et al. 1994). Based on the structure, the rotational catalysis was experimentally proven by a variety of biochemical and spectroscopic techniques. Most convincingly, the rotation of a micrometer-sized fluorescent actin filament attached to the central shaft  $\gamma$  subunit has been directly visualized by video microscopy of single F<sub>1</sub> molecules (Noji et al. 1997). Rotation was also observed when the actin filament was attached to subunit  $\epsilon$  or to the c<sub>10–15</sub> oligomer (Kato-Yamada et al. 1998; Pänke et al. 2000; Sambongi et al. 1999; Tsonuda et al. 2001). These studies confirmed several cross-linking studies, which have been important to define subunits  $\gamma$ ,  $\epsilon$ , and c<sub>10–15</sub> as the rotor subunits and subunits  $\alpha_3$ ,  $\beta_3\delta$ , a, and b<sub>2</sub> as the stator subunits (Capaldi et al. 2000). It was found that cross-links between subunits  $\gamma$ ,  $\epsilon$ , and c did not block ATP-driven proton translocation, whereas cross-links between subunits  $\gamma$  or  $\epsilon$  and  $\alpha$  or  $\beta$  led to an inhibition of the enzyme. Consistent with these data is a medium-resolution electron density map of an F<sub>1</sub> complex from yeast with an attached c<sub>10</sub> ring, which shows a physical connection between the  $\gamma$  and  $\epsilon$  subunits and the c ring at its cytoplasmic loops (Stock et al. 1999).

Single-molecule experiments with small magnetic or gold beads or with fluorescent dyes instead of the large actin filament provided insights into mechanistic details of the enzyme. Rotation in the fully coupled Na<sup>+</sup>-ATP synthase was observed both in synthesis and hydrolysis mode (Kaim et al. 2002).

Rotation of the rotor was counterclockwise in the ATP hydrolysis direction and clockwise in the ATP synthesis direction, when viewed from the  $F_0$  domain (Diez et al. 2004; Itoh et al. 2004), and performed up to 700 revolutions per second (Nakanishi-Matsui et al. 2006). In  $F_1$ , the  $\gamma$  subunit rotates in steps of  $120^\circ$  for each ATP molecule hydrolyzed. Each  $120^\circ$  step can be further divided into four stages. In the ATP binding dwell, an ATP molecule binds to the empty  $\beta_1$  site and elicits a rapid  $80^\circ$  substep rotation of the  $\gamma$  subunit. In the following catalytic dwell, ATP is thought to be cleaved at the  $\beta_2$  site and ADP and/or phosphate is released from the  $\beta_3$  site. This initiates a  $40^\circ$  substep rotation of the  $\gamma$  subunit completing its  $120^\circ$  rotation (Yasuda et al. 2001; Nishizaka et al. 2004; Shimabukuru et al. 2003). The rotational behavior of  $F_1F_0$  resembled that of  $F_1$ , indicating that friction in the  $F_0$  motor is negligible during ATP-driven rotation. Tributyltin chloride, a specific inhibitor of the ion access route in subunit a (von Ballmoos et al. 2004), inhibited rotation by 96% (Ueno et al. 2005), in accordance with strict coupling between mechanical and ion translocation events. When the performance of the  $F_1$  motor was probed by sophisticated single-molecule experiments in femtoliter-sized chambers, the hydrolysis of three ATP molecules per revolution was directly observed and showed very high mechanochemical coupling (Rondelez et al. 2005). If the  $\gamma$  subunit of  $F_1$  was forced to rotate in the ATP synthesis direction, ATP synthesis from ADP and phosphate was observed. Interestingly, the mechanochemical coupling efficiency was low for an  $F_1$  subcomplex lacking the  $\epsilon$  subunit, but reached more than 70% after the reconstitution with this protein (Rondelez et al. 2005). The  $\epsilon$  subunit thus has an important role in the synthesis of ATP, but the mechanism for this function has not yet been elucidated.

### 4.3

#### The $F_0$ Motor

The  $F_0$  motor is a membrane-bound protein complex consisting of an oligomeric ring of c subunits, a single a subunit, and a dimer of b subunits, which flank the c ring laterally (Mellwig and Böttcher 2003; Rubinstein et al. 2003). Early on, the c subunit has attracted much interest, because of its very hydrophobic character and its small size, which facilitated its purification by extraction into organic solvent mixtures. Based on amino acid sequencing and specific labeling studies with a hydrophobic diazirine derivative, subunit c was predicted to fold as a helical hairpin, consisting of two membrane spanning  $\alpha$  helices and a cytoplasmic connecting loop (Hoppe et al. 1984). Importantly, the C-terminal  $\alpha$  helix contains a conserved acidic residue, approximately in the middle of the membrane, which plays a profound role in proton translocation. Accordingly, mutagenesis of the respective aspartic acidic residue in *E. coli* (D61) to asparagine, or its chemical substitution with the specific F-ATPase inhibitor dicyclohexylcarbodiimide (DCCD), results in the impairment of proton translocation (Hoppe et al. 1982; Sebald et al. 1980). Hence, the D61 residues

are thought to extract protons from one and deliver them to the other side of the membrane, as the c ring rotates. Accordingly, the  $F_0$  motor of *P. modestum*, which conducts  $\text{Na}^+$ , harbors specific binding sites for  $\text{Na}^+$  on its c ring (Kluge and Dimroth 1992; Kaim et al. 1997). Biochemical evidence for these sites was obtained by DCCD labeling experiments (Kluge and Dimroth 1993a,b; 1994). The ATP synthase of *P. modestum* was specifically labeled at cE65, which is equivalent to cD61 of *E. coli*. The chemical modification with DCCD consumes a proton, and consequently the reaction rate increased from alkaline to acidic pH values, following a titration curve with an apparent pK of 6.5, which reflects the pK of cE65 (Kluge and Dimroth 1993a). Importantly,  $\text{Na}^+$  ions protected from this modification and shifted the pK of cE65 into the acidic range, indicating a competition of  $\text{Na}^+$  and  $\text{H}^+$  binding to the same site.

The  $\text{Na}^+$  binding sites on the c ring were confirmed by mutational studies. First, random mutagenesis of the c ring and selection for  $\text{Na}^+$ -independent growth on succinate minimal medium led to the identification of a double mutant in subunit c, which abolished  $\text{Na}^+$  binding and made the holoenzyme to a more efficient  $\text{H}^+$ -translocating ATP synthase (Kaim and Dimroth 1995). As these c-subunit mutations are near the C terminus, in considerable distance to the ion binding glutamate 65, they must exert their effect via a long-distance conformational change at the binding site. Second, using site-specific mutagenesis, the  $\text{Na}^+$  binding site was identified to be contributed by the triad cQ32, cE65, and cS66 (Kaim et al. 1997). These three residues are conserved in all  $\text{Na}^+$ -translocating  $F_1F_0$  ATP synthases. In the high-resolution structure of the c ring from *I. tartaricus*, the side chains of these three amino acids were indeed seen to be  $\text{Na}^+$  binding ligands (Meier et al. 2005). The topography of the binding site within the middle of the membrane was identified by photocross-linking experiments using a photoactivatable DCCD derivative attached to cE65 (von Ballmoos et al. 2002a). This became specifically bound to the fatty acid side chains of the phospholipids. Quenching experiments with a fluorescent DCCD derivative attached to cE65 and phospholipids carrying a spin label at different positions of the fatty acid side chains were consistent with this membrane location (von Ballmoos et al. 2002b).

#### 4.4

##### Subunit C Structures

Two different structures of the *E. coli* c subunit were solved by NMR at pH 5 and 8, respectively, in an organic solvent mixture (Girvin et al. 1998; Rastogi and Girvin 1999). In the pH 5 structure, which is thought to present the conformation during exposure to the lipids, D61 has an inward facing orientation. In the pH 8 structure, however, which is thought to represent the conformation in the interface with subunit a, D61 is exposed to the surface. The latter conformation matches cross-linking data between subunits c and a (Jiang and Fillingame 1998). To account for these results, a c ring model



was proposed, in which the C-terminal helix performs a large 140° swiveling versus the N-terminal helix (Fillingame et al. 2003) in the interface with subunit a. This relocates the proton binding D61 to the surface to permit loading or unloading of the site from and to subunit a. NMR investigations of the *P. modestum* c subunit revealed different secondary structures in SDS and in the organic solvent mixture, and neither was similar to one of the *E. coli* c subunit structures (Matthey et al. 1999, 2002). Therefore, an artifactual folding of the protein due to the unphysiological environment of a c monomer in an organic solvent mixture or a harsh detergent could not be excluded.

In the native ATP synthase, the c subunits assemble into an oligomeric ring, the stoichiometry of which varies depending on the species. Rings with ten monomers exist in yeast mitochondria (Stock et al. 1999), the thermophilic bacterium PS3 (Mitome et al. 2004), and possibly in *E. coli* (Jiang et al. 2001), whereas rings found in the bacterium *I. tartaricus* (Stahlberg et al. 2001) and *P. modestum* (Meier et al. 2003) have 11 monomers. The archaeon *Methanopyrus kandleri* harbors a gene in which 13 c subunits are fused (Lolkema et al. 2003), suggesting that this organism produces a corresponding ring with 13 fused c subunits. Furthermore, ring stoichiometries of 14 and 15 have been found in chloroplasts (Seelert et al. 2000) and the cyanobacterium *Spirulina platensis* (Pogoryelov et al. 2005), respectively. An even larger ring with 20 hairpins resulting from ten double-size subunits and harboring ten ion binding sites exists in the V-type ATPase from *Enterococcus hirae* (Murata et al. 2005). The number of subunits in each ring also indicates the number of ions transported across the membrane during each cycle of the ATP synthase. Consequently, as the F<sub>1</sub> motor contains three catalytic sites and synthesizes three molecules of ATP per cycle, a variation in the number of c subunits and ion binding sites automatically leads to different H<sup>+</sup> (Na<sup>+</sup>) to ATP ratios. ATP synthases with large c rings have a high H<sup>+</sup> (Na<sup>+</sup>) to ATP ratio, which would be advantageous for ATP synthesis at low ion motive force. Conversely, ATP synthases with small c rings might prevail in organisms with constantly high ion motive force: the low H<sup>+</sup> (Na<sup>+</sup>) to ATP ratio of these enzymes results in a more efficient use of energy. A mismatch to the threefold symmetry of the F<sub>1</sub> motor created by F<sub>0</sub> motors with 10, 11, 13, or 14 c subunits has been regarded as functionally important (Stock et al. 1999; Murata et al. 2004) in order to prevent the enzyme from becoming trapped in deep energy minima. However, recent data from the c<sub>15</sub> ring of the *S. platensis* ATP synthase show that symmetry mismatch is not mandatory for function (Pogoryelov et al. 2005).

#### 4.5

##### Structure of the C Ring From *I. tartaricus*

The Na<sup>+</sup>-translocating ATP synthases of *P. modestum* or *I. tartaricus* have the distinct advantage of containing an oligomeric c ring of excessive stabil-

ity (Laubinger and Dimroth 1988; Neumann et al. 1998; Meier and Dimroth 2002). This facilitated the purification of the c ring from the *I. tartaricus* ATP synthase in high yield and purity (Meier et al. 2003). The isolated c ring could be reconstituted with subunits a and b to form a functional  $F_0$  moiety, indicating that it retained its native conformation (Wehrle et al. 2002a). The initial investigations on the c ring structure were performed by atomic force microscopy and electron microscopy after reconstitution into lipid vesicles and crystallization in two dimensions (Stahlberg et al. 2001; Meier et al. 2003). The structure was solved at medium resolution (4 Å) by electron crystallography (Vonck et al. 2002) and at high resolution (2.4 Å) by X-ray crystallography (Meier et al. 2004) (Fig. 5). In the structure of the oligomer, each c ring is composed of 11 subunits. Of these, each monomer is folded as a helical hairpin with the loop at the cytoplasmic side and the termini at the periplasmic side, as was predicted earlier by independent methods (Girvin et al. 1998; Hoppe et al. 1984). The structure (Fig. 5) shows a cylindrical, hourglass-shaped protein complex which has a height of  $\sim 70$  Å and protrudes from the membrane on either side. Its outer diameter is  $\sim 40$  Å in the middle and  $\sim 50$  Å at the top

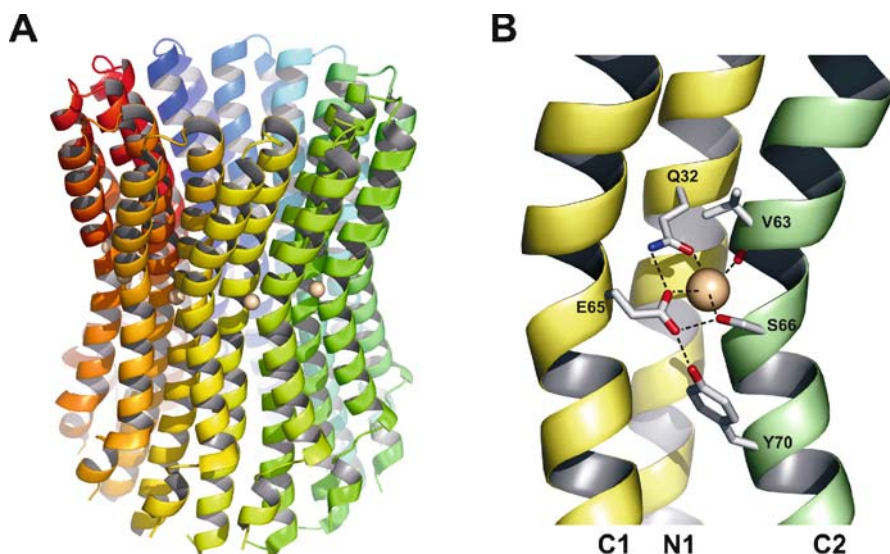


**Fig. 5** Structure of the *I. tartaricus*  $c_{11}$  ring in ribbon form. **A** Individual subunits are shown in different colors. The *spheres* indicate the bound  $\text{Na}^+$  ions. **B** Close-up of the  $\text{Na}^+$  binding site formed by the inner (N1) and outer helix (C1) of one c subunit and the outer helix (C2) of the neighboring c subunit.  $\text{Na}^+$  coordination and selected hydrogen bonds are indicated with *dashed lines*. The structure shows the locked conformation. During opening, the side chain of Y70 might relocate into a cavity underneath the binding site, thus destabilizing the hydrogen-bonding network and allowing unloading and loading of the binding site to and from subunit a

and bottom. The 11 N-terminal helices are closely spaced within an inner ring surrounding a cavity of  $\sim 17$  Å. The tight helix packing leaves no space for side chains and is accounted for by a highly conserved motif of four glycine residues in the inner, N-terminal helix (Vonck et al. 2002). Each N-terminal helix is connected to a C-terminal helix by a loop formed by the highly conserved peptide R45, N46, P47 which is exposed to the cytoplasmic surface (Watts et al. 1995; Hermolin et al. 1999). The C-terminal helices pack into the grooves formed between N-terminal helices, producing the outer ring. All helices show a bend of about  $20^\circ$  in the middle of the membrane (at P28 and E65 in the N-terminal and C-terminal helices, respectively) causing the narrow part of the hourglass shape. Moreover, the bend tilts the helices in the cytoplasmic half out of the plane by  $\sim 10^\circ$ , yielding a right-handed twisted packing. When the c ring is viewed from the cytoplasm, it rotates counter-clockwise during ATP synthesis against the drag imposed by the  $F_1$  motor components. Thus, the resulting torque might decrease the bend and increase the interhelical distance in the cytoplasmic part of the c ring, depending on the energies involved. Such a conformational change under load might serve to store elastic energy in the c ring, adding to that described for the central and peripheral stalk subunits (Junge et al. 2001). The internal surface of the c ring is very hydrophobic and was shown by photocross-linking experiments to be filled with phospholipids in the natural environment of the membrane (Oberfeld et al. 2006).

Perhaps the most instructive feature of the c ring structure is the arrangement of the  $\text{Na}^+$  binding sites. Eleven bound  $\text{Na}^+$  ions are seen in the c ring structure near the middle of the membrane facing toward the outer surface of the c ring (Fig. 5) (Meier et al. 2004), which confirms previous cross-linking data (von Ballmoos et al. 2002a). Each of the 11  $\text{Na}^+$  ions is bound at the interface of an N-terminal and two C-terminal helices. The coordination sphere is formed by side chain oxygen atoms of Q32 and E65 of one subunit and the side chain oxygen atom of S66 and the backbone carbonyl oxygen atom of V63 of the neighboring subunit (Fig. 5). An intriguing observation is that E65 acts not only as one of the  $\text{Na}^+$  binding ligands but also as the recipient of hydrogen bonds from the side chains of Q32, S66, and Y70. This arrangement generates a stable, locked conformation of the binding site, from which the horizontal transfer of  $\text{Na}^+$  to subunit a is prevented. This implies that the present locked conformation of the binding site converts to an open one at the subunit a/c interface in order to allow the horizontal ion transfer to and from subunit a.

The a subunit abuts the c ring laterally and is implicated in providing access to the ion binding site at the c subunit in the subunit a/c interface from either one or both sides of the membrane, depending on the model. Subunit a is an extremely hydrophobic protein containing five to six transmembrane helices (Jäger et al. 1998; Long et al. 1998; Valiyaveetil and Fillingame 1998). Of particular interest is the interface of the a subunit with the c ring, which

has to guarantee the stability of the a/c complex while allowing an almost frictionless rotation between these protein components, as revealed by single-molecule experiments (Ueno et al. 2005). These peculiarities have impeded structural determinations of subunit a. So far, biochemical and mutational studies suggest that the universally conserved aR226 residue (*P. modestum* numbering), which is localized approximately at the same level in the membrane as the cE65, is important in ion translocation.

## 5

### Mechanism of the $F_0$ Motor

#### 5.1

##### The Proton Motor

The  $F_0$  motor converts the energy stored in an electrochemical ion gradient into mechanical rotation. Hence, the torque generating mechanism is an integral part of the transport of the coupling ions across the membrane. Theoretical considerations and a large body of experimental data have led to the proposal of several models for the  $F_0$  motor function, which are considerably distinct in detail but share common features as well (Aksimentiev et al. 2004; Feniouk et al. 2004; Xing et al. 2004). The initial model of the  $H^+$ -driven motor of the *E. coli* ATP synthase (Junge et al. 1997; Vik and Antonio 1994) predicts that only a protonated, uncharged cD61 site can move from the subunit a/c interface into the lipid phase. To account for sufficient torque generation and to prevent proton leakage in the subunit a/c interface, the initial model was extended by positioning the essential positive stator arginine between the access and the exit pathway of the ion (Elston et al. 1998). The model predicts that inlet and outlet channels are located in a noncoaxial manner in subunit a (Fig. 6). The ion is proposed to enter the site through the inlet channel from the low-pH reservoir and to exit through the outlet channel into the high-pH reservoir, after performing an almost complete rotation. The unprotonated site is located between the two channels, and without an external driving force the motor is in an idling mode, and the site shuttles between the channels with equal probability to either side. In the presence of a  $\Delta pH$ , the proton concentration in each of the separate aqueous access channels is unequal, and the site will be protonated more frequently at the position of the channel with higher proton concentration. The protonated site is now able to move out of the a/c subunit interface into the lipid phase. Simultaneously, a new site enters the interface, where its ion is displaced by the stator arginine. The negatively charged empty site acts as a ratchet, due to the large energy penalty of its backward movement into the lipid phase. In this model, the pH gradient determines the direction of rotation and simultaneously acts as the main driving force for the generation of torque.

## Zones in the a/c interface

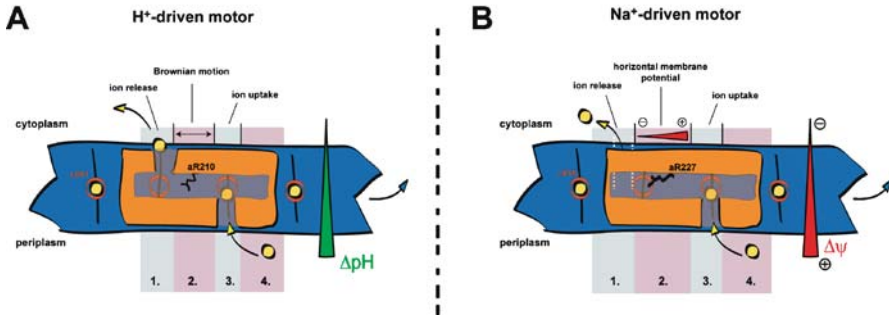


**Fig. 6** Model for torque generation in the  $H^+$ - and  $Na^+$ -translocating  $F_0$  motor. **A** Two-channel model with a ratchet-type mechanism for  $H^+$ -dependent enzymes. The crucial events during ion translocation in ATP synthesis direction in the a/c interface can be divided into four zones. (1) The occupied rotor site enters the interface and releases its coupling ion through the outlet channel into the cytoplasm with high pH. Deprotonation prevents the backward rotation into the lipid phase acting as a molecular ratchet. (2) The negative charge of the binding site is compensated by the stator arginine. In this functionally symmetric state, Brownian back and forth motions toward either channel are possible. (3) As the inlet channel, which is in contact with the periplasm where the pH is low, contains more protons than the outlet channel, which is in contact with the cytoplasm, the binding site is more frequently protonated from the periplasm. Therefore, the  $\Delta pH$  determines the direction of rotation. (4) The loaded binding site can now move out of the interface into the lipid bilayer, whereby the next binding site enters the interface and experiences the events described in (1). **B** Push-and-pull model for  $Na^+$ -dependent enzymes. (1) In ATP synthesis direction, an occupied rotor site enters the interface from the left and releases its bound  $Na^+$  ion toward the cytoplasm. This process is aided by the stator arginine. (2) The arginine compensates for the now negatively charged empty site. The horizontal component of the membrane potential, however, pulls the arginine to the left and pushes the glutamate to the right. Therefore, the electrical component of the ion motive force determines the direction of rotation from left to right. (3) The hydration of the binding site within the inlet channel stabilizes this conformation and allows loading of the binding site from the periplasm. Movement of the binding site from zone 2 to 3 pulls the next rotor site into the a/c interface as described in (1). (4) The binding site that has been occupied from the periplasm is allowed to rotate out of the interface into the lipid phase. The event is aided by a push mechanism during the events described in (2)

Experiments with engineered cysteines within helices II, IV, and V show good accessibility of these residues from the periplasmic side to approximately the middle of the membrane, which would be in accord with a periplasmic inlet channel. From the cytoplasmic surface, cysteines were only accessible within helix IV, and those cysteines were very close to the membrane surface (Angevine and Fillingame 2003; Angevine et al. 2003). Conclusive evidence for a cytoplasmic access channel within subunit a is therefore not available so far.

## 5.2

### The Sodium Motor

In contrast to the proton-translocating ATP synthases, where the path of the ion across the membrane is intrinsically difficult to establish, the  $\text{Na}^+$ -translocating counterparts provide unique experimental options for these investigations. For example, (1)  $\text{Na}^+$  concentrations on either side of the membrane can be manipulated at will without compromising the stability of the enzyme, (2)  $\text{Na}^+$  translocation can be conveniently measured with the radioactive isotope  $^{22}\text{Na}^+$  (Dimroth 1982b) or with a  $\text{Na}^+$ -binding fluorophore (von Ballmoos and Dimroth 2004), and (3) screening methods can be used to select for mutants with impaired or modified  $\text{Na}^+$  binding characteristics. Many details of the ion translocation through the  $\text{F}_0$  motor and of the mechanical rotation connected to it have therefore been explored with the  $\text{Na}^+$ -translocating ATP synthase of *P. modestum*. These experiments support a model where the ion binding sites on the c ring are accessible from the periplasmic surface through a corridor in subunit a, and from the cytoplasmic surface through a route that is either c ring-intrinsic or within the interface between the c ring and subunit a (Dimroth et al. 2006).

#### 5.2.1

##### The Ion Path

In the following we will describe some of the experiments that have led to the model of the sodium  $\text{F}_0$  motor and we will then give a detailed description of this model. *E. coli* deletion mutants in the *atp* operon are unable to grow on a nonfermentable carbon source such as succinate. This defect could be complemented by expressing the *E. coli*  $\text{F}_1$  ( $-\delta$ ) together with the *P. modestum*  $\text{F}_0$  ( $+\delta$ ) genes on a plasmid and thus allowed the construction and investigation of mutants in the  $\text{F}_0$  genes of the  $\text{Na}^+$ -dependent enzyme (Kaim and Dimroth 1993, 1994). The parent *E. coli*/*P. modestum* hybrid ATP synthase showed the same  $\text{Na}^+$ -dependent growth characteristics as the  $\text{F}_1\text{F}_0$  ATP synthase of *P. modestum*. In a random mutagenesis approach, mutants with a  $\text{Na}^+$ -independent growth phenotype could be isolated, which could be grouped into two categories. Mutants of the first category contained a double mutation in the C-terminal tail of subunit c (Kaim and Dimroth 1995). The mutation affected the geometry of the binding site in such a way that  $\text{Na}^+$  ions were no longer able to bind, whereas the ability for  $\text{Li}^+$  or  $\text{H}^+$  binding was retained. The second group of mutants contained a triple mutation in subunit a, which affected the ion specificity of the periplasmic access route to the binding site, so that  $\text{Na}^+$  access was abolished whereas  $\text{Li}^+$  or  $\text{H}^+$  access was retained (Kaim and Dimroth 1998a). The mutant cells could grow on succinate only in the absence, but not in the presence, of  $\text{Na}^+$  ions, suggesting that sodium ions were unable to get access to the binding

site through the periplasmic entrance channel, and simultaneously prevented protons from reaching the binding sites via this route. Furthermore,  $\text{Na}^+$  ions inhibited the ATP hydrolysis activity of the mutant ATP synthase, and one  $\text{Na}^+$  per  $\text{F}_1\text{F}_0$  became firmly occluded in the subunit a/c interface after ATP addition (Kaim et al. 1998; Kaim and Dimroth 1998a). Hence, after ATP-driven rotation of the binding site into the interface, any further rotation is prevented if the  $\text{Na}^+$  ion cannot be released from the binding site into the periplasm due to blockage of this route by the subunit a triple mutation. Besides by mutation, the periplasmic access route for  $\text{Na}^+$  was also blocked by the inhibitor tributyltin chloride (von Ballmoos et al. 2004). A photoactivatable derivative of this compound was found to specifically label subunit a. Sodium ions were protected from this labeling, indicating a competition between tributyltin chloride and  $\text{Na}^+$  for the binding at the same site. The most obvious candidate for this site is the  $\text{Na}^+$  access pathway. This supposition is in accord with biochemical data, showing that tributyltin chloride not only blocks the hydrolysis of ATP, but also transport of sodium ions across the membrane.

So far, neither inhibitors nor mutants have been found for the cytoplasmic access route to the binding site, and it is not resolved as to whether this route is localized entirely in the c ring or in the interface between the c ring and subunit a. Although several lines of evidence compellingly demonstrate that cytoplasmic access to the binding site can occur outside the subunit a/c interface in a time scale of seconds (von Ballmoos et al. 2002; Meier et al. 2003), it is not certain whether this ion path can account for physiological rates in the millisecond timescale. Among these evidences are (1) the demonstration of  $\text{Na}^+$  or  $\text{H}^+$  binding to the c subunit sites within the isolated c ring; (2) ATP-driven occlusion of  $^{22}\text{Na}^+$  by the a subunit triple mutant, even after partial modification of the c ring with DCCD (Kaim and Dimroth 1998b)—this observation compulsorily requires that the radioactive  $^{22}\text{Na}^+$  enters a site between the DCCD-modified c subunit and the a subunit; and (3) the exchange of  $\text{Na}^+$  between both sides of the membrane with partially DCCD-modified c subunits (Kaim and Dimroth 1998b). This result requires shuttling of the rotor between the periplasmic access channel in the subunit a/c interface and a position outside the a/c interface, where the ions must exchange between the cytoplasm and the binding site.

### 5.2.2

#### The Driving Force

Experiments have also been performed to determine the driving forces required for torque generation. According to Mitchell's chemiosmotic hypothesis, the chemical concentration gradient of the coupling ion and the membrane potential contribute equally to the driving force in a system at thermodynamic equilibrium. However, under physiological conditions, far from

thermodynamic equilibrium, each individual component can contribute kinetically unequally to the driving force. It was found that in the absence of external energy, the  $F_0$  motor, either isolated or connected to the  $F_1$  motor, performs an idling motion of the rotor versus the stator, which causes  $\text{Na}^+$  ions to exchange between the exterior and interior compartments separated by the membrane (Kluge and Dimroth 1992; Kaim and Dimroth 1998b). Exchange by the isolated  $F_0$  motor is not converted into unidirectional rotation coupled to unidirectional ion flux by applying large  $\text{Na}^+$  concentration gradients, but only with a threshold membrane potential of about 40 mV (Kluge and Dimroth 1992; Dimroth et al. 2003). Hence, the membrane potential is the kinetically indispensable driving force for torque generation and cannot be compensated by a  $\text{Na}^+$  concentration gradient. These results were corroborated by ATP synthesis experiments with reconstituted ATP synthases from *P. modestum*, *E. coli*, or chloroplasts. With each of these enzymes, ATP synthesis was only observed after applying a certain membrane potential and not with large  $\text{Na}^+$  or  $\text{H}^+$  concentration gradients (Kaim and Dimroth 1999).

It is clear that the principal torque generating and ion translocation events occur in the subunit a/c interface, and it would therefore be of great interest to learn more about the critical parts of this protein assembly. As mentioned above, probably the most important residue for function in subunit a is the universally conserved arginine 226 (*P. modestum* numbering) near the middle of the penultimate transmembrane helix. Mutants of this residue in the *P. modestum* a subunit have provided important insights into its role for the operation of the  $F_0$  motor (Wehrle et al. 2002b). All the evidence is consistent with an attribution of the positively charged residue to repel the  $\text{Na}^+$  ions from approaching binding sites into the appropriately positioned release route to either the periplasmic or the cytoplasmic surface, depending on the direction of rotation. The most conservative R226K mutant was completely inactive in ATP-driven ion transport at pH 7.0, similar to the corresponding *E. coli* mutant (Valiyaveetil and Fillingame 1997), but interestingly attained catalytic power between pH 8 and 9. In the R226H mutation, the activity profile was shifted into the acidic range, with maximal activities between pH 6.5 and 7.5. ATP synthase with an R226A substitution catalyzed  $\text{Na}^+$ -dependent ATP hydrolysis, which was completely inhibited by DCCD, but not coupled to  $\text{Na}^+$  transport. Taken together, these results suggest that a positive charge at position 226 is necessary to accomplish the dissociation of the  $\text{Na}^+$  ions from approaching rotor sites. Furthermore, an arginine with its delocalized positive charge appears to be better suited for an unrestricted diffusion of the negatively charged empty rotor site than a lysine with a positive point charge. Hence, at neutral pH, when the lysine is completely protonated, it electrostatically attracts a negatively charged rotor site so powerfully that the charge has to be attenuated by its partial deprotonation at higher pH values, in order for the rotor site to escape.



### 5.2.3

#### The Model for Torque Generation

On the basis of these experimental data, a model for torque generation by the  $\text{Na}^+$ -translocating  $\text{F}_0$  motor was proposed which is in accordance with mathematical calculations (Dimroth et al. 1999, 2006; Xing et al. 2004). In this model, the binding sites in the rotor/stator interface have to interact in a coordinated manner with the coupling ion, the positive stator charge (R226), and the membrane potential, as shown schematically in Fig. 6 for the ATP synthesis direction. During its journey through the interface with the stator, a rotor site moves along a sequence of states as follows (Xing et al. 2004). As the occupied site (site 1) enters the a/c interface, it is in the vicinity of the positive stator charge, which forces the bound sodium ion to dissociate. The negative charge of site 1 is now compensated by the positive stator charge. In the idling mode, when no external energy source is applied, the rotor can shuttle back and forth against the stator up to a certain angle. However, in the presence of a membrane potential (cytoplasmic negative), the movement becomes directional (see below), bringing the empty site 1 in juxtaposition with the periplasmic access route of subunit a. Upon hydration of the site, the free energy drops to trap it at its present position, until a  $\text{Na}^+$  ion has been bound. So far the movement of site 1 has simultaneously pulled the next occupied rotor site (site 2) into the a/c interface. Site 2 now follows the same events as site 1 before, to release its  $\text{Na}^+$  ion and to be pulled into juxtaposition with the stator charge, and this movement pushes the occupied site 1 out of the interface into the lipid phase. Accordingly, two rotor sites operate together in a push and pull fashion to achieve rotation of the rotor versus the stator.

To account for the essence of the membrane potential for torque generation (see above), it can be assumed that only part of it drops vertically between the periplasmic channel entrance and its terminus in the middle of the membrane and that between the latter and the terminus of the cytoplasmic access route, the membrane potential drops in a horizontal direction. This horizontal potential causes the stator charge to orient toward the incoming rotor sites and the charged rotor site to become attracted to the periplasmic entrance channel. Hence, the membrane potential acts as the main kinetic driving force for unidirectional rotation and ATP synthesis.

The  $\text{Na}^+$  and the  $\text{H}^+$  motors are distinct in their use of the ion release pathway, which is thought to be located in subunit a in the proton motor, whereas evidence now suggests the presence of an ion release pathway in the c ring of the sodium motor. The other main difference is in the energy source that drives each  $\text{F}_0$  motor out of the relaxed, idling mode into unidirectional rotation to produce torque. Apart from these differences, both models are similar. Each motor operating in the direction of ATP synthesis performs a molecular cycle, in which a specific binding site on the c ring captures a coupling ion from the side with high electrochemical potential and releases it to the side

with low electrochemical potential. As loading and unloading of the binding site can only be accomplished at defined positions at the subunit a/c interface, ion translocation is closely connected to the rotation of the c ring. Hence, the mechanical rotation is linked to the ion translocation events in the  $F_0$  motor components, and is transmitted through the camshaft-like rotating central stalk into the ATP synthesizing  $F_1$  motor.

**Acknowledgements** We wish to thank Pius Dahinden for preparing Figs. 2 and 3. Work in the authors' laboratory was supported by the Swiss National Science Foundation and by the Forschungskommission der ETH Zürich.

## References

- Abrahams JP, Leslie AG, Lutter R, Walker JE (1994) Structure at 2.8 Å resolution of  $F_1$ -ATPase from bovine heart mitochondria. *Nature* 370:621–628
- Aksimentiev A, Balabin IA, Fillingame RH, Schulten K (2004) Insight into the molecular mechanism of rotation in the  $F_0$  sector of ATP synthase. *Biophys J* 86:1332–1344
- Angevine CM, Fillingame RH (2003) Aqueous access channels in subunit a of rotary ATP synthase. *J Biol Chem* 278:6066–6074
- Angevine CM, Herold KA, Fillingame RH (2003) Aqueous access pathways in subunit a of rotary ATP synthase extend to both sides of the membrane. *Proc Natl Acad Sci USA* 100:13179–13183
- Berg M, Dimroth P (1998) The biotin protein MadF of the malonate decarboxylase from *Malonomonas rubra*. *Arch Microbiol* 170:464–468
- Berg M, Hilbi H, Dimroth P (1996) The acyl carrier protein of malonate decarboxylase of *Malonomonas rubra* contains 2'-(5''-phosphoribosyl)-3'-dephosphocoenzyme A as a prosthetic group. *Biochemistry* 35:4689–4696
- Berg M, Hilbi H, Dimroth P (1997) Sequence of a gene cluster from *Malonomonas rubra* encoding components of the malonate decarboxylase  $Na^+$  pump and evidence for their function. *Eur J Biochem* 245:103–115
- Bott M (1997) Anaerobic citrate metabolism and its regulation in enterobacteria. *Arch Microbiol* 167:78–88
- Bott M, Dimroth P (1994) *Klebsiella pneumoniae* genes for citrate lyase and citrate lyase ligase: localization, sequencing and expression. *Mol Microbiol* 14:347–356
- Bott M, Meyer M, Dimroth P (1995) Regulation of anaerobic citrate metabolism in *Klebsiella pneumoniae*. *Mol Microbiol* 18:533–546
- Bott M, Pfister K, Burda P, Kalbermatter O, Woehlke G, Dimroth P (1997) Methylmalonyl-CoA decarboxylase from *Propionigenium modestum*: cloning and sequencing of the structural genes and purification of the enzyme complex. *Eur J Biochem* 250:590–599
- Boyer PD (1993) The binding change mechanism for ATP synthase—some probabilities and possibilities. *Biochim Biophys Acta* 1140:215–250
- Buckel W (2001). Sodium ion-translocating decarboxylases. *Biochim Biophys Acta* 1505:15–27
- Buckel W, Semmler R (1983) Purification, characterisation and reconstitution of glutacyl-CoA decarboxylase, a biotin-dependent sodium pump from anaerobic bacteria. *Eur J Biochem* 136:427–434
- Busch W, Saier MH Jr (2002) The transporter classification (TC) system, 2002. *Crit Rev Biochem Mol Biol* 37:287–337

- Capaldi RA, Aggeler R (2002) Mechanism of the  $F_1F_0$ -type ATP synthase, a biological rotary motor. *Trends Biochem Sci* 27:154–160
- Capaldi RA, Schulenberg B, Murray J, Aggeler R (2000) Cross-linking and electron microscopy studies of the structure and functioning of the *Escherichia coli* ATP synthase. *J Exp Biol* 203(Pt1):29–33
- Dahinden P, Dimroth P (2004) Oxaloacetate decarboxylase of *Archaeoglobus fulgidus*: cloning of genes and expression in *Escherichia coli*. *Arch Microbiol* 182:414–420
- Dahinden P, Auchli Y, Granjon T, Taralczak M, Wild M, Dimroth P (2005a) Oxaloacetate decarboxylase of *Vibrio cholerae*: purification, characterization, and expression of the genes in *Escherichia coli*. *Arch Microbiol* 183:121–129
- Dahinden P, Pos KM, Taralczak M, Dimroth P (2005b) Identification of a domain in the  $\alpha$ -subunit of the oxaloacetate decarboxylase  $Na^+$  pump that accomplishes complex formation with the  $\gamma$ -subunit. *FEBS J* 272:846–855
- Dehning I, Schink B (1989) *Malonomonas rubra* gen. nov., sp. nov., a microaerotolerant anaerobic bacterium growing by decarboxylation of malonate. *Arch Microbiol* 151:427–433
- Denger K, Schink B (1982) Energy conservation by succinate decarboxylation in *Veillonella parvula*. *J Gen Microbiol* 138:967–971
- DiBerardino M, Dimroth P (1995) Synthesis of the oxaloacetate decarboxylase  $Na^+$  pump and its individual subunits in *Escherichia coli* and analysis of their function. *Eur J Biochem* 231:790–801
- DiBerardino M, Dimroth P (1996) Aspartate 203 of the oxaloacetate decarboxylase  $\beta$ -subunit catalyses both the chemical and vectorial reaction of the  $Na^+$  pump. *EMBO J* 15:1842–1849
- Diez M, Zimmermann B, Börsch M, König M, Schweinberger E, Steigmiller S, Reuter R, Felekyan S, Kudryavtsev V, Seidel CA, Gräber P (2004) Proton-powered subunit rotation in single membrane-bound  $F_0F_1$ -ATP synthase. *Nat Struct Mol Biol* 11:135–141
- Dimroth P (1980) A new sodium-transport system energized by the decarboxylation of oxaloacetate. *FEBS Lett* 122:234–236
- Dimroth P (1982a) The role of biotin and sodium in the decarboxylation of oxaloacetate by the membrane-bound oxaloacetate decarboxylase from *Klebsiella aerogenes*. *Eur J Biochem* 121:435–441
- Dimroth P (1982b) The generation of an electrochemical gradient of sodium ions upon decarboxylation of oxaloacetate by the membrane-bound and  $Na^+$ -activated oxaloacetate decarboxylase from *Klebsiella aerogenes*. *Eur J Biochem* 121:443–449
- Dimroth P (1997) Primary sodium ion translocating enzymes. *Biochim Biophys Acta* 1318:11–51
- Dimroth P (2004) Molecular basis for bacterial growth on citrate or malonate. In: Curtiss R (ed) *EcoSal—Escherichia coli and Salmonella: cellular and molecular biology*. ASM, Washington, DC, chap. 3.4.6
- Dimroth P, Cook GM (2004) Bacterial  $Na^+$ - or  $H^+$ -coupled ATP synthases operating at low electrochemical potential. *Adv Microb Physiol* 49:175–218
- Dimroth P, Hilbi H (1997) Enzymic and genetic basis for bacterial growth on malonate. *Mol Microbiol* 25:3–10
- Dimroth P, Schink B (1998) Energy conservation in the decarboxylation of dicarboxylic acids by fermenting bacteria. *Arch Microbiol* 170:69–77
- Dimroth P, Thomer A (1983) Subunit composition of oxaloacetate decarboxylase and characterization of the alpha chain as carboxyltransferase. *Eur J Biochem* 137:107–112
- Dimroth P, Thomer A (1993) On the mechanism of sodium ion translocation by oxaloacetate decarboxylase of *Klebsiella pneumoniae*. *Biochemistry* 32:1734–1739

- Dimroth P, Wang H, Grabe M, Oster G (1999) Energy transduction in the sodium F-ATPase of *Propionigenium modestum*. Proc Natl Acad Sci USA 96:4924–4929
- Dimroth P, von Ballmoos C, Meier T, Kaim G (2003) Electrical power fuels rotary ATP synthase. Structure (Camb) 11:1469–1473
- Dimroth P, von Ballmoos C, Meier T (2006) Catalytic and mechanical cycles in F-ATP synthases. Fourth in the cycles review series. EMBO Rep 7:276–282
- Elston T, Wang H, Oster G (1998) Energy transduction in ATP synthase. Nature 391:510–513
- Feniouk BA, Kozlova MA, Knorre DA, Cherepanov DA, Mulkidjanian AY, Junge W (2004) The proton-driven rotor of ATP synthase: ohmic conductance (10 fS) and absence of voltage gating. Biophys J 86:4094–4109
- Ferguson SA, Keis S, Cook GM (2006) Biochemical and molecular characterization of a Na<sup>+</sup>-translocating F<sub>1</sub>F<sub>0</sub> ATPase from the thermoalkaliphilic bacterium *Clostridium paradoxum*. J Bacteriol 188:5045–5054
- Fillingame RH, Angevine CM, Dmitriev OY (2003) Mechanics of coupling proton movements to c-ring rotation in ATP synthase. FEBS Lett 555:29–34
- Gay NJ (1984) Construction and characterization of an *Escherichia coli* strain with a *uncI* mutation. J Bacteriol 158:820–825
- Girvin ME, Rastogi VK, Abildgaard F, Markley JL, Fillingame RH (1998) Solution structure of the transmembrane H<sup>+</sup>-transporting subunit c of the F<sub>1</sub>F<sub>0</sub> ATP synthase. Biochemistry 37:8817–8824
- Hall PR, Zheng R, Lizamma A, Pusztai-Carey M, Carey PR, Lee VC (2004) Transcarboxylase 5 S structures: assembly and catalytic mechanism of a multienzyme complex subunit. EMBO J 23:3621–3631
- Hermolin J, Dmitriev OY, Zhang Y, Fillingame RH (1999) Defining the domain of binding of F<sub>1</sub> subunit  $\epsilon$  with the polar loop of F<sub>0</sub> subunit c in the *Escherichia coli* ATP synthase. J Biol Chem 274:17011–17016
- Hilbi H, Dehning I, Schink B, Dimroth P (1992) Malonate decarboxylase of *Malonomonas rubra*, a novel type of biotin-containing acetyl enzyme. Eur J Biochem 207:117–123
- Hilpert W, Dimroth P (1982) Conversion of the chemical energy of methylmalonyl-CoA decarboxylation into a Na<sup>+</sup> gradient. Nature 296:584–585
- Hilpert W, Dimroth P (1983) Purification and characterization of a new sodium-transport decarboxylase. Methylmalonyl-CoA decarboxylase from *Veillonella alcalescens*. Eur J Biochem 132:579–587
- Hilpert W, Dimroth P (1991) On the mechanism of sodium ion translocation by methylmalonyl-CoA decarboxylase from *Veillonella alcalescens*. Eur J Biochem 19:79–86
- Hilpert W, Schink B, Dimroth P (1984) Life by a new decarboxylation-dependent energy conservation mechanism with Na<sup>+</sup> as coupling ion. EMBO J 3:1665–1670
- Hoppe J, Scheirer HU, Friedl P, Sebald W (1982) An Asp–Asn substitution in the proteolipid subunit of the ATP synthase from *Escherichia coli* leads to a non-functional proton channel. FEBS Lett 145:21–29
- Hoppe J, Brunner J, Joergensen BB (1984) Structure of the membrane-embedded F<sub>0</sub> part of F<sub>1</sub>F<sub>0</sub> ATP synthase from *Escherichia coli* as inferred from labeling with 3-(trifluoromethyl)-3-(*m*-[<sup>125</sup>I]iodophenyl)diazirine. Biochemistry 23:5610–5616
- Huder JB, Dimroth P (1993) Sequence of the sodium ion pump methylmalonyl-CoA decarboxylase from *Veillonella parvula*. J Biol Chem 268:24564–24571
- Itoh H, Takahashi A, Adachi K, Noji H, Yasuda R, Yoshida M, Kinoshita K Jr (2004) Mechanically driven ATP synthesis by F<sub>1</sub>-ATPase. Nature 427:465–468
- Jäger H, Birkenhäger R, Stalz W-D, Altendorf K, Deckers-Hebestreit G (1998) Topology of subunit a of the *Escherichia coli* ATP synthase. Eur J Biochem 251:122–132

- Jiang W, Fillingame RH (1988) Interacting helical faces of subunit a and c in the  $F_1F_0$  ATP synthase of *Escherichia coli* defined by disulfide cross-linking. *Proc Natl Acad Sci USA* 95:6607–6612
- Jiang W, Hermolin J, Fillingame RH (2001) The preferred stoichiometry of c subunits in the rotary motor sector of *Escherichia coli* ATP synthase is 10. *Proc Natl Acad Sci USA* 98:4966–4971
- Jockel P, Di Berardino M, Dimroth P (1999) Membrane topology of the  $\beta$  subunit of the oxaloacetate decarboxylase  $Na^+$  pump from *Klebsiella pneumoniae*. *Biochemistry* 38:13461–13472
- Jockel P, Schmid M, Choinowski T, Dimroth P (2000a) Essential role of tyrosine 229 of the oxaloacetate decarboxylase beta-subunit in the energy coupling mechanism of the  $Na^+$  pump. *Biochemistry* 39:4320–4326
- Jockel P, Schmid M, Steuber J, Dimroth P (2000b) A molecular coupling mechanism for the oxaloacetate decarboxylase  $Na^+$  pump as inferred from mutational analysis. *Biochemistry* 39:2307–2315
- Junge W, Lill H, Engelbrecht S (1997) ATP synthase: an electrochemical transducer with rotatory mechanics. *Trends Biochem Sci* 22:420–423
- Junge W, Pänke O, Cherepanov DA, Gumbiowski K, Müller M, Engelbrecht S (2001) Inter-subunit rotation and elastic power transmission in  $F_0F_1$  ATPase. *FEBS Lett* 504:152–160
- Kaim G, Dimroth P (1993) Formation of a functionally active sodium-translocating  $F_1F_0$  ATPase in *Escherichia coli* by homologous recombination. *Eur J Biochem* 218:937–944
- Kaim G, Dimroth P (1994) Construction, expression and characterization of a plasmid-encoded  $Na^+$ -specific ATPase hybrid consisting of *Propionigenium modestum*  $F_0$ -ATPase and *Escherichia coli*  $F_1$ -ATPase. *Eur J Biochem* 222:615–623
- Kaim G, Dimroth P (1995) A double mutation in subunit c of the  $Na^+$ -specific  $F_1F_0$  ATPase of *Propionigenium modestum* results in a switch from  $Na^+$ - to  $H^+$ -coupled ATP synthesis in the *Escherichia coli* host cells. *J Mol Biol* 253:726–738
- Kaim G, Dimroth P (1998a) A triple mutation in the a subunit of the *Escherichia coli*/*Propionigenium modestum*  $F_1F_0$  ATPase hybrid causes a switch from  $Na^+$  stimulation to  $Na^+$  inhibition. *Biochemistry* 37:4626–4634
- Kaim G, Dimroth P (1998b) Voltage-generated torque drives the motor of the ATP synthase. *EMBO J* 17:5887–5895
- Kaim G, Dimroth P (1999) ATP synthesis by F-type ATP synthase is obligatorily dependent on the transmembrane voltage. *EMBO J* 18:4118–4127
- Kaim G, Ludwig W, Dimroth P, Schleifer KH (1992) Cloning, sequencing and in vivo expression of genes encoding the  $F_0$  part of the sodium-ion-dependent ATP synthase of *Propionigenium modestum* in *Escherichia coli*. *Eur J Biochem* 207:463–470
- Kaim G, Wehrle F, Gerike U, Dimroth P (1997) Molecular basis for the coupling ion selectivity of  $F_1F_0$  ATP synthases: probing the liganding groups for  $Na^+$  and  $Li^+$  in the c subunit of the ATP synthase from *Propionigenium modestum*. *Biochemistry* 36:9185–9194
- Kaim G, Matthey U, Dimroth P (1998) Mode of interaction of the single a subunit with the multimeric c subunits during the translocation of the coupling ions by  $F_1F_0$  ATPases. *EMBO J* 17:688–695
- Kaim G, Prummer M, Sick B, Zumofen G, Renn A, Wild UP, Dimroth P (2002) Coupled rotation within single  $F_0F_1$  enzyme complexes during ATP synthesis or hydrolysis. *FEBS Lett* 525:156–163
- Kato-Yamada Y, Noji H, Yasuda R, Kinosita K, Yoshida M (1998) Direct observation of the rotation of the  $\epsilon$  subunit in  $F_1$ -ATPase. *J Biol Chem* 273:19375–19377

- Kluge C, Dimroth P (1992) Studies on Na<sup>+</sup> and H<sup>+</sup> translocation through the F<sub>0</sub> part of the Na<sup>+</sup>-translocating F<sub>1</sub>F<sub>0</sub> ATPase from *Propionigenium modestum*: discovery of a membrane potential dependent step. *Biochemistry* 31:12665–12672
- Kluge C, Dimroth P (1993a) Kinetics of inactivation of the F<sub>1</sub>F<sub>0</sub> ATPase of *Propionigenium modestum* by dicyclohexylcarbodiimide in relationship to H<sup>+</sup> and Na<sup>+</sup> concentration: probing the binding site for the coupling ions. *Biochemistry* 32:10378–10386
- Kluge C, Dimroth P (1993b) Specific protection by Na<sup>+</sup> and Li<sup>+</sup> of the F<sub>1</sub>F<sub>0</sub> ATPase of *Propionigenium modestum* from the reaction with dicyclohexylcarbodiimide. *J Biol Chem* 268:14557–14560
- Kluge C, Dimroth P (1994) Modification of isolated subunit c of the F<sub>1</sub>F<sub>0</sub>-ATPase from *Propionigenium modestum* by dicyclohexylcarbodiimide. *FEBS Lett* 340:245–248
- Krumholz LR, Esser U, Simoni RD (1992) Characterization of the genes coding for the F<sub>1</sub>F<sub>0</sub> subunits of the sodium dependent ATPase of *Propionigenium modestum*. *FEMS Microbiol Lett* 91:37–42
- Laubinger W, Dimroth P (1987) Characterization of the Na<sup>+</sup>-stimulated ATPase of *Propionigenium modestum* as an enzyme of the F<sub>1</sub>F<sub>0</sub> type. *Eur J Biochem* 168:475–480
- Laubinger W, Dimroth P (1988) Characterization of the ATP synthase of *Propionigenium modestum* as a primary sodium pump. *Biochemistry* 27:7531–7537
- Laubinger W, Dimroth P (1989) The sodium ion translocating adenosinetriphosphatase of *Propionigenium modestum* pumps protons at low sodium ion concentrations. *Biochemistry* 28:7194–7198
- Lolkema JS, Boekema EJ (2003) The A-type ATP synthase subunit K of *Methanopyrus kandleri* is deduced from its sequence to form a monomeric rotor comprising 13 hairpin domains. *FEBS Lett* 543:47–50
- Long JC, Wang S, Vik SB (1998) Membrane topology of subunit a of the F<sub>1</sub>F<sub>0</sub> ATP synthase as determined by labeling of unique cysteine residues. *J Biol Chem* 273:16235–16240
- Matthey U, Kaim G, Braun D, Wüthrich K, Dimroth P (1999) NMR studies of subunit c of the ATP synthase from *Propionigenium modestum* in dodecylsulfate micelles. *Eur J Biochem* 261:459–467
- Matthey U, Braun D, Dimroth P (2002) NMR investigations of subunit c of the ATP synthase from *Propionigenium modestum* in chloroform/methanol/water (4 : 4 : 1). *Eur J Biochem* 269:1942–1946
- Matthies C, Schink B (1992a) Energy conservation in fermentative glutarate degradation by the bacterial strain WoGl3. *FEMS Microbiol Lett* 79:221–225
- Matthies C, Schink B (1992b) Reciprocal isomerization of butyrate and isobutyrate by the strictly anaerobic bacterium strain WoGl3 and methanogenic isobutyrate degradation by a defined triculture. *Appl Environ Microbiol* 58:1435–1439
- Matthies C, Springer N, Ludwig W, Schink B (2000) *Pelospira glutarica* gen. nov., sp. nov., a glutarate-fermenting, strictly anaerobic, spore-forming bacterium. *Int J Syst Evol Microbiol* 50(Pt2):645–648
- Meier T, Dimroth P (2002) Intersubunit bridging by Na<sup>+</sup> ions as a rationale for the unusual stability of the c-rings of Na<sup>+</sup>-translocating F<sub>1</sub>F<sub>0</sub> ATP synthases. *EMBO Rep* 3:1094–1098
- Meier T, Matthey U, von Ballmoos C, Vonck J, Krug von Nidda T, Kühlbrandt W, Dimroth P (2003) Evidence for structural integrity in the undecameric c-rings isolated from sodium ATP synthases. *J Mol Biol* 325:389–397
- Meier T, Polzer P, Diederichs K, Welte W, Dimroth P (2005) Structure of the rotor ring of F-type Na<sup>+</sup>-ATPase from *Ilyobacter tartaricus*. *Science* 308:659–662
- Mellwig C, Böttcher B (2003) A unique resting position of the ATP synthase from chloroplasts. *J Biol Chem* 278:18544–18549

- Mitome N, Suzuki T, Hayashi S, Yoshida M (2004) Thermophilic ATP synthase has a decamer c ring: indication of noninteger 10 : 3 H<sup>+</sup>/ATP ratio and permissive elastic coupling. *Proc Natl Acad Sci USA* 101:12159–12164
- Müller V, Aufurth S, Rahlfs S (2001) The Na<sup>+</sup> cycle in *Acetobacterium woodii*: identification and characterization of a Na<sup>+</sup>-translocating F<sub>1</sub>F<sub>0</sub>-ATPase with a mixed oligomer of 8 and 16 kDa proteolipids. *Biochim Biophys Acta* 1505:108–120
- Murata T, Yamato I, Kakinuma Y, Leslie AG, Walker JE (2005) Structure of the rotor of the V-type Na<sup>+</sup>-ATPase from *Enterococcus hirae*. *Science* 308:654–659
- Nakanishi-Matsui M, Kashiwagi S, Hosokawa H, Cipriano DJ, Dunn SD, Wada Y, Futai M (2006) Stochastic high-speed rotation of *Escherichia coli* ATP synthase F<sub>1</sub> sector: the epsilon subunit sensitive rotation. *J Biol Chem* 281:4126–4131
- Neumann S, Matthey U, Kaim G, Dimroth P (1998) Purification and properties of the F<sub>1</sub>F<sub>0</sub> ATPase of *Ilyobacter tartaricus*, a sodium ion pump. *J Bacteriol* 180:3312–3316
- Nishizaka T, Oiwa K, Noji H, Kimura S, Muneyuki E, Yoshida M, Kinoshita K Jr (2004) Chemomechanical coupling in F<sub>1</sub>-ATPase revealed by simultaneous observation of nucleotide kinetics and rotation. *Nat Struct Mol Biol* 11:142–148
- Noji H, Yasuda R, Yoshida M, Kinoshita K (1997) Direct observation of the rotation of F<sub>1</sub> ATPase. *Nature* 386:299–302
- Oberfeld B, Brunner J, Dimroth P (2006) Phospholipids occupy the internal lumen of the c ring of the ATP synthase of *Escherichia coli*. *Biochemistry* 45:1841–1851
- Pänke O, Gumbiowski K, Junge W, Engelbrecht S (2000) F-ATPase: specific observation of the rotating c subunit oligomer of EF<sub>0</sub>EF<sub>1</sub>. *FEBS Lett* 472:34–38
- Pogoryelov D, Yu J, Meier T, Vonck J, Dimroth P, Müller DJ (2005) The c<sub>15</sub> ring of the *Spirulina platensis* F-ATP synthase: F<sub>1</sub>F<sub>0</sub> symmetry mismatch is not obligatory. *EMBO Rep* 6:5474–5483
- Pos KM, Dimroth P (1996) Functional properties of the purified Na<sup>+</sup>-dependent citrate carrier of *Klebsiella pneumoniae*: evidence for asymmetric orientation of the carrier in proteoliposomes. *Biochemistry* 35:1018–1026
- Rastogi VK, Girvin ME (1999) Structural changes linked to proton translocation by subunit c of the ATP synthase. *Nature* 402:263–268
- Rondelez Y, Tresset G, Nakashima T, Kato-Yamada Y, Fujita H, Takeuchi S, Noji H (2005) Highly coupled ATP synthesis by F<sub>1</sub> single molecules. *Nature* 433:773–777
- Rubinstein JL, Walker JE, Henderson R (2003) Structure of the mitochondrial ATP synthase by electron cryomicroscopy. *EMBO J* 22:6182–6192
- Sambongi Y, Iko Y, Tanabe M, Omote H, Iwamoto-Kihara A, Ueda I, Yanagida T, Wada Y, Futai M (1999) Mechanical rotation of the c subunit oligomer in ATP synthase F<sub>1</sub>F<sub>0</sub>: direct observation. *Science* 286:1722–1724
- Schaffitzel C, Berg M, Dimroth P, Pos KM (1998) Identification of an Na<sup>+</sup>-dependent malonate transporter of *Malonomonas rubra* and its dependence on two separate genes. *J Bacteriol* 180:2689–2693
- Shink B, Pfennig N (1982) *Propionigenium modestum* gen. nov. sp. nov., a new strictly anaerobic, nonsporing bacterium growing on succinate. *Arch Microbiol* 133:209–216
- Schmid M, Wild M, Dahinden P, Dimroth P (2002a) Subunit  $\gamma$  of the oxaloacetate decarboxylase Na<sup>+</sup> pump: interaction with other subunits/domains of the complex and binding site for the Zn<sup>2+</sup> metal ion. *Biochemistry* 41:1285–1292
- Schmid M, Vorburger T, Pos KM, Dimroth P (2002b) Role of conserved residues within helices IV and VIII of the oxaloacetate decarboxylase  $\beta$  subunit in the energy coupling mechanism of the Na<sup>+</sup> pump. *Eur J Biochem* 269:2997–3004
- Schneider K, Dimroth P, Bott M (2000a) Biosynthesis of the prosthetic group of citrate lyase. *Biochemistry* 39:9438–9450



- Schneider K, Dimroth P, Bott M (2000b) Identification of triphosphoribosyl-dephospho-CoA as precursor of the citrate lyase prosthetic group. *FEBS Lett* 483:165–168
- Schneider K, Kästner CN, Meyer M, Wessel M, Dimroth P, Bott M (2002) Identification of a gene cluster in *Klebsiella pneumoniae* which includes *citX*, a gene required for biosynthesis of the citrate lyase prosthetic group. *J Bacteriol* 184:2439–2446
- Sebald W, Machleidt W, Wachter E (1980) *N,N'*-dicyclohexylcarbodiimide binds specifically to a single glutamyl residue of the proteolipid subunit of the mitochondrial adenosinetriphosphatase from *Neurospora crassa* and *Saccharomyces cerevisiae*. *Proc Natl Acad Sci USA* 77:785–789
- Seelert H, Poetsch A, Dencher NA, Engel A, Stahlberg H, Müller DJ (2000) Proton-powered turbine of a plant motor. *Nature* 405:418–419
- Shimabukuro K, Yasuda R, Muneyuki E, Hara KY, Kinoshita K Jr, Yoshida M (2003) Catalysis and rotation of  $F_1$  motor: cleavage of ATP at the catalytic site occurs in 1 ms before 40 degree substep rotation. *Proc Natl Acad Sci USA* 100:13731–13736
- Stahlberg H, Müller DJ, Suda K, Fotiadis D, Engel A, Meier T, Matthey U, Dimroth P (2001) Bacterial  $Na^+$ -ATP synthase has an undecameric rotor. *EMBO Rep* 2:229–233
- Steuber J, Krebs W, Bott M, Dimroth P (1999) A membrane-bound  $NAD(P)^+$ -reducing hydrogenase provides reduced pyridine nucleotides during citrate fermentation by *Klebsiella pneumoniae*. *J Bacteriol* 181:241–245
- Stock D, Leslie AG, Walker JE (1999) Molecular architecture of the rotary motor in ATP synthase. *Science* 286:1700–1705
- Studer R, Dahinden P, Wang W-W, Auchli Y, Li X-D, Dimroth P (2007) Crystal structure of the carboxyltransferase domain of the oxaloacetate decarboxylase  $Na^+$  pump from *Vibrio cholerae*. *J Mol Biol* 367:547–557
- Thauer RK, Jungermann K, Decker K (1977) Energy conservation in chemotrophic anaerobic bacteria. *Bacteriol Rev* 41:100–180
- Tsunoda SP, Aggeler R, Yoshida M, Capaldi RA (2001) Rotation of the c subunit oligomer in fully functional  $F_1F_0$  ATP synthase. *Proc Natl Acad Sci USA* 98:898–902
- Ueno H, Suzuki T, Kinoshita K Jr, Yoshida M (2005) ATP-driven stepwise rotation of  $F_0F_1$ -ATP synthase. *Proc Natl Acad Sci USA* 102:1333–1338
- Valiyaveetil FI, Fillingame RH (1997) On the role of Arg-210 and Glu-219 on subunit a in proton translocation by the *Escherichia coli*  $F_1F_0$  ATP synthase. *J Biol Chem* 272:32635–32641
- Valiyaveetil FI, Fillingame RH (1998) Transmembrane topography of subunit a in the *Escherichia coli*  $F_1F_0$  ATP synthase. *J Biol Chem* 273:16241–16247
- Vik SB, Antonio BJ (1994) A mechanism of proton translocation by  $F_1F_0$  ATP synthase suggested by double mutants of the a subunit. *J Biol Chem* 269:30364–30369
- von Ballmoos C, Dimroth P (2004) A continuous fluorescent method for measuring  $Na^+$  transport. *Anal Biochem* 335:334–337
- von Ballmoos C, Appoldt Y, Brunner J, Granier T, Vasella A, Dimroth P (2002a) Membrane topography of the coupling ion binding site in  $Na^+$ -translocating  $F_1F_0$  ATP synthase. *J Biol Chem* 277:3504–3510
- von Ballmoos C, Meier T, Dimroth P (2002b) Membrane embedded location of  $Na^+$  or  $H^+$  binding sites on the rotor ring of  $F_1F_0$  ATP synthases. *Eur J Biochem* 269:5581–5589
- von Ballmoos C, Brunner J, Dimroth P (2004) The ion channel of F-ATP synthase is the target of toxic organotin compounds. *Proc Natl Acad Sci USA* 101:11239–11244
- Vonck J, von Nidda TK, Meier T, Matthey U, Mills DJ, Kühlbrandt W, Dimroth P (2002) Molecular architecture of the undecameric rotor of a bacterial  $Na^+$ -ATP synthase. *J Mol Biol* 321:307–316



- Watts SD, Zhang Y, Fillingame RH, Capaldi RA (1995) The gamma subunit in the *Escherichia coli* ATP synthase complex (ECF<sub>1</sub>F<sub>0</sub>) extends through the stalk and contacts the c subunit of the F<sub>0</sub> part. FEBS Lett 368:235–238
- Wehrle F, Appoldt Y, Kaim G, Dimroth P (2002a) Reconstitution of F<sub>0</sub> of the sodium ion translocating ATP synthase of *Propionigenium modestum* from its heterologously expressed and purified subunits. Eur J Biochem 269:2567–2573
- Wehrle F, Kaim G, Dimroth P (2002b) Molecular mechanism of the ATP synthase's F<sub>0</sub> motor probed by mutational analyses of subunit a. J Mol Biol 322:369–381
- Wendt KS, Schall I, Huber R, Buckel W, Jacob U (2003) Crystal structure of the carboxyltransferase subunit of the bacterial sodium ion pump glutaconyl-coenzyme A decarboxylase. EMBO J 22:3493–3502
- Wifling K, Dimroth P (1989) Isolation and characterization of oxaloacetate decarboxylase of *Salmonella typhimurium*, a sodium pump. Arch Microbiol 152:584–588
- Wild MR, Pos KM, Dimroth P (2003) Site-directed sulfhydryl labeling of the oxaloacetate decarboxylase Na<sup>+</sup> pump of *Klebsiella pneumoniae*: helix VIII comprises a portion of the sodium ion channel. Biochemistry 42:11615–11624
- Woehlke G, Dimroth P (1994) Anaerobic growth of *Salmonella typhimurium* on L(+)- and D(-)-tartrate involves an oxaloacetate decarboxylase Na<sup>+</sup> pump. Arch Microbiol 162:233–237
- Woehlke G, Wifling K, Dimroth P (1992) Sequence of the sodium ion pump oxaloacetate decarboxylase from *Salmonella typhimurium*. J Biol Chem 267:22798–22803
- Xing J, Wang H, von Ballmoos C, Dimroth P, Oster G (2004) Torque generation by the F<sub>0</sub> motor of the sodium ATPase. Biophys J 87:2148–2163
- Yasuda R, Noji H, Yoshida M, Kinosita K Jr, Itoh H (2001) Resolution of distinct rotational substeps by submillisecond kinetic analysis of F<sub>1</sub>-ATPase. Nature 410:898–904